NRIM SR–93–02

Basic Fatigue Properties of JIS Steels for Machine Structural Use

by

Satoshi NISHIJIMA

NRIM Special Report
(Technical Report)
No. 93–02

1 9 9 3

National Research Institute for Metals
2–3–12 Nakameguro, Meguroku, Tokyo, Japan

NRIM SR-93-02

Basic Fatigue Properties of JIS Steels for Machine Structural Use

by

Satoshi NISHIJIMA

NRIM Special Report
(Technical Report)
No. 93-02

1993

National Research Institute for Metals
2-3-12 Nakameguro, Meguroku, Tokyo, Japan

Basic Fatigue Properties of JIS Steels for Machine Structural Use

by

Satoshi NISHIJIMA

NRIM Special Report
(Technical Report)
No. 93–02

Contents

Basic Fatigue Properties of JIS Steels for Machine Structural Use

by

Satoshi NISHIJIMA*

Abstract

This paper intends to provide Standard Reference Data on the basic high-cycle fatigue strengths of current Japanese steels and alloys which are designated in the Japanese Industrial Standards (JIS) and most commonly used for mechanical structures. In total 162 individual heats of 15 different grades of carbon, low-alloy and stainless steels were sampled from ordinary products of representative manufacturers in the country. Chemical composition was controlled at the materials sampling with the intent to have wide-spread values in quench hardenability and thus to cover the range of variations to be expected in JIS materials.

The materials were then heat treated and fatigue tested at the National Research Institute for Metals (NRIM) according to the standardized procedures. Fatigue strengths were evaluated under rotating bending, reversed torsion and axial loading. More than 12,000 standard smooth specimens were fatigue tested at room temperature in laboratory air and 667 *S-N* curves were statistically determined for different materials and loading conditions.

The analyzed data is correlated with basic enginneering properties such as hardness, tensile and impact values of materials. Some typical dependence of the fatigue strength on the microscopic defects and on the cyclic stress-strain properties are discussed. Primary test data have already been published as NRIM Fatigue Data Sheets and available on request on exchange basis.

Keywords: *Fatigue of metals, NRIM Fatigue Data Sheet, JIS steels, High-cycle fatigue, Heat treatments, Mechanical properties, Non-metallic inclusions, cyclic yield strength*

* Director, Failure Physics Division, NRIM.

1. Introduction

The aim of the present paper is to provide Standard Reference Data on the basic high-cycle fatigue strengths of current Japanese steels and alloys. The materials are all those designated in the Japanese Industrial Standards (JIS) and most commonly used for mechanical structures. The data cited here are based on the nation-wide testing program to establish Standard Fatigue Data on Engineering Materials in Japan[1], conducted since 1975 at the National Research Institute for Metals (NRIM).

The primary data from this program have been published periodically as NRIM Fatigue Data Sheets (FDS), and distributed worldwide on exchange basis. It would be better to explain briefly about the FDS Project, before entering further in detail.

Background of the NRIM FDS goes back to early in the 1960's, where NRIM was at the accomplishment of the first 7-year program of investment since its foundation. There was a keen demand from industries to establish a national materials testing center which could supply high quality and neutral data for Japanese materials. It was needed to help solidifying the basis of safe and reliable use of Japanese materials for machines and structures.

The project was widely supported from academic, industrial and governmental people, and NRIM engaged in the preparation to play such a role. A series of Long-Term Creep Testing was at first initiated at NRIM in 1966 using more than 1100 testing machines. Another series of Fatigue Testing was started in 1975 with 78 different testing facilities which have various load capacities ranging from 50 kN to 1.5 MN.

Outline of the NRIM Fatigue Data Sheet Program is described elsewhere[1].

NRIM FDS Project includes three subthemes:

(1) Basic strength-life properties of machine structural materials

(2) Life and crack growth properties of welded structural steels, and

(3) Time-dependent strain-life properties of high-temperature alloys

The scope of the Project implies establishment of common basic fatigue data referable for materials fabricators as well as for materials users. An Advisory Committee was settled at NRIM to reflect opinions of leading scientists and engineers in universities and industries in the orientation of Project. Three Technical Advisory Subcommittees were also formed to review in detail individual test programs and acquired data with specialists from industries of various fields.

The present paper is related to only a part of the first subtheme mentioned above and deals specifically with basic high-cycle fatigue properties at room temperature of carbon, low alloy and stainless steels. Direct reference of the original FDS publications[2–16] is recommended.

Topics not thoroughly treated here such as low-cycle fatigue[17–22] or crack growth properties will be appeared in the subsequent publications of NRIM Special Report. More comprehensive representation of analyzed data in this paper can be found in NRIM FDS Technical Reports in Japanese[23,24].

2. Materials Sampling and Test Procedures

2.1 Test Materials

Table 1 lists the materials sampled and tested for the FDS which are cited in this paper. There are 7 types of steels, such as carbon, Mn, Cr-Mo, Ni-Cr, Ni-Cr-Mo and stainless steels, pertaining to 15 classes of steels and consisting of 162 heats/lots of materials.

They were successively sampled in 1975–80 from ordinary products of representative Japanese steel manufacturers, as hot rolled round bars, generally of 19–22 mm in diameter. There were a few exception in size for some heats of SNCM439 samples, which were about 50 mm and hot rolled to size in NRIM. All of them were killed ingot steels produced by LD converter (LDC) or basic electric arc (BEA) furnaces of different capacities, as indicated in the table.

The sampling was carried out according to the following principle:

- Consider as population a whole of ordinary products from representive manufacturers in the country whose total market share covers a major part of the JIS steel grade in question
- Divide the range of JIS chemical composition for the steel grade into high, medium and low sub-classes, looking at the quench hardenabil-

Table 1. Typical chemical composition and fabrication history of the test materials (sampled in 1975–80)

Steel	Typical composition	Furnace (t)	Ingot (t)	Dia (mm)	Heat
S25C	0.25C	LDC/BEA 15–110	2.5–6.3	19–22	11
S35C	0.35C	LDC/BEA 15–110	2.5–6.3	19–22	12
S45C	0.45C	LDC/BEA 15–110	2.5–6.3	19–22	11
S55C	0.55C	LDC/BEA 15–110	2.5–6.3	19–22	11
SMn438	0.38C-1.5Mn	LDC/BEA 10–80	2.5–6.0	19–23	7
SMn443	0.43C-1.5Mn	LDC/BEA 10–86	2.5–6.5	19–23	12
SCr440	0.40C-1Cr	LDC/BEA 10–80	2.5–6.5	19–22	8
SCM435	0.35C-1Cr-0.2Mo	LDC/BEA 30–80	2.5–6.5	19–22	14
SCM440	0.40C-1Cr-0.2Mo	LDC/BEA 10–80	2.5–6.5	19–22	15
SNC631	0.31C-2.7Ni-0.8Cr	LDC/BEA 10–80	1.2–6.0	19–22	10
SNCM439	0.39C-1.8Ni-0.8Cr-0.2Mo	BEA 10–80	1.2–5.4	19–22	14
SNCM447	0.47C-1.8Ni-0.8Cr-0.2Mo	BEA 10–30	2.5	19–20	6
SUS403	12Cr	BEA 10–60	2.5–5.3	19–22	11
SUS430	17Cr	BEA 30–60	2.2–3.4	19–22	9
SUS304	18Cr-8Ni	BEA 10–60	2.5–3.4	19–22	11

ity, and select arbitrarily one heat/lot of steel per sub-class from each manufacturer, and
- Sample on average 12 individual heats/lots of steels for one grade considering annual testing capability

The sub-division of chemical composition was made in order that the sampled materials would reflect the range of scatter in population, given that they are specified by the chemical composition with certain allowance. More detailed comment will be given later in this paper. One direct example for explanation is the case of carbon steels, where the range of carbon content was divided into three. This allowed to classify the samples from a same JIS grade to those having upper, middle and lower carbon concentrations, which normally exhibit systematically different hardness after quenching.

The grades of steels in Table 1 were selected as they were known to be the most commonly used in mechanical industries, normally at heat-treated states, because of the importance of their fatigue performance. There are still many other special steels and alloys which have to be considered in fatigue designing. Some of them are actually tested in FDS grogram, as those of case hardened steels, spring and tool steels and aluminum alloys. However, those data will be analyzed and reported separately, as their quality and use are very different from the present ones.

Table 2 lists the chemical composition of each steel by ladle analysis, comparing the respective JIS requirement and the results for the test materials. No particular comment is necessary, except, perhaps, for intentionally lower content of expensive elements such as Mo for some steels.

2.2 Heat Treatments

Test materials were succeedingly cut into pieces of about 200 mm in length and heat treated at NRIM, so as to prepare necessary speciments for each heat/lot of steels. The heat treatment was designed according to the following principle:
- Normalization, quenching, and tempering are to be carried out for carbon and low alloy steels, whereas annealing or solution treatment is applied for ferritic and austenitic stainless steels, respectively, as in ordinary usage of steels.
- Temperature for the treatments is selected from typical values that are most commonly agreed

Table 2. Chemical composition requested in JIS (upper) and the materials tested (lower), for ladle analysis in mass %

Steel	C	Si	Mn	100P	100S	Ni	Cr	Mo	100Cu
S25C	0.22–0.28 0.22–0.28	0.15–0.35 0.16–0.32	0.30–0.60 0.37–0.52	≦3.0 ≦2.6	≦3.5 ≦2.8	≦0.20 ≦0.07	≦0.20 ≦0.17	— —	≦30 ≦10
S35C	0.32–0.38 0.32–0.38	0.15–0.35 0.20–0.30	0.60–0.90 0.63–0.81	≦3.0 ≦2.6	≦3.5 ≦3.0	≦0.20 ≦0.07	≦0.20 ≦0.12	— —	≦30 ≦12
S45C	0.42–0.48 0.42–0.48	0.15–0.35 0.20–0.27	0.60–0.90 0.67–0.80	≦3.0 ≦2.8	≦3.5 ≦2.3	≦0.20 ≦0.05	≦0.20 ≦0.12	— —	≦30 ≦15
S55C	0.52–0.58 0.52–0.57	0.15–0.35 0.21–0.32	0.60–0.90 0.67–0.84	≦3.0 ≦2.4	≦3.5 ≦2.6	≦0.20 ≦0.06	≦0.20 ≦0.14	— —	≦30 ≦22
SMn438	0.35–0.41 0.34–0.40	0.15–0.35 0.22–0.27	1.35–1.65 1.40–1.59	≦3.0 ≦2.3	≦3.0 ≦2.0	≦0.25 ≦0.06	≦0.35 ≦0.22	— —	≦30 ≦ 9
SMn443	0.40–0.41 0.40–0.46	0.15–0.35 0.22–0.32	1.35–1.65 1.40–1.60	≦3.0 ≦2.7	≦3.0 ≦2.2	≦0.25 ≦0.10	≦0.35 ≦0.27	— —	≦30 ≦10
SCr440	0.38–0.43 0.39–0.42	0.15–0.35 0.22–0.31	0.60–0.85 0.72–0.79	≦3.0 ≦1.9	≦3.0 ≦1.3	≦0.25 ≦0.06	0.90–1.20 0.96–1.13	— —	≦30 ≦13
SCM435	0.33–0.38 0.33–0.38	0.15–0.35 0.23–0.35	0.60–0.85 0.68–0.81	≦3.0 ≦2.5	≦3.0 ≦2.7	≦0.25 ≦0.12	0.90–1.20 0.96–1.09	0.15–0.30 0.15–0.19	≦30 ≦18
SCM440	0.38–0.43 0.38–0.43	0.15–0.35 0.22–0.29	0.60–0.85 0.69–0.85	≦3.0 ≦2.4	≦3.0 ≦2.3	≦0.25 ≦0.23	0.90–1.20 0.96–1.11	0.15–0.30 0.15–0.22	≦30 ≦15
SNC631	0.27–0.35 0.28–0.35	0.15–0.35 0.23–0.31	0.35–0.65 0.50–0.65	≦3.0 ≦2.0	≦3.0 ≦1.6	2.50–3.50 2.62–2.84	0.60–1.00 0.72–0.94	— —	≦30 ≦13
SNCM439	0.36–0.43 0.37–0.43	0.15–0.35 0.21–0.32	0.60–0.90 0.66–0.79	≦3.0 ≦2.3	≦3.0 ≦2.4	1.60–2.00 1.63–1.92	0.60–1.00 0.69–0.92	0.15–0.30 0.16–0.26	≦30 ≦13
SNCM447	0.44–0.50 0.44–0.48	0.15–0.35 0.18–0.29	0.60–0.90 0.69–0.82	≦3.0 ≦1.5	≦3.0 ≦1.7	1.60–2.00 1.66–1.80	0.60–1.00 0.73–0.81	0.15–0.30 0.17–0.21	≦30 ≦11
SUS403	≦0.15 0.09–0.15	≦0.50 0.19–0.50	≦1.00 0.31–0.85	≦4.0 ≦2.9	≦3.0 ≦2.2	≦0.60 0.08–0.29	11.5–13.0 11.7–12.8	— 0.02–0.15	
SUS430	≦0.12 0.06–0.10	≦0.75 0.30–0.59	≦1.00 0.39–0.69	≦4.0 ≦3.9	≦3.0 ≦1.6	— 0.20–0.35	16.0–18.0 16.1–17.6	— 0.01–0.09	
SUS304	≦0.08 0.05–0.08	≦1.00 0.33–0.83	≦2.00 0.69–1.78	≦4.5 ≦3.6	≦3.0 ≦2.8	8.00–11.5 8.3–10.28	18.0–20.0 18.2–19.6	— 0.07–0.32	

for respective types of steels. Tempering is to be performed at higher, middle and lower temperatures of the range most popularly used for the steel grade.

- All the treatments are conducted at NRIM using salt baths, with a batch consisting of 24 pieces of cut materials, of arbitrarily chosen 3 heats and with 8 pieces per heat.
- Statistical care is to be taken at every steps of work not to introduce unexpected bias in the results

Table 3 gives the condition of heat treatment applied to the test materials. As the result, typical low carbon steel S25C was only normalized, ferritic

Table 3. Heat treatment temperatures in °C with air cooling (AC), water quenching (WQ), oil quenching (OQ) or water cooling (WC)

Steel	Normalizing 30 min hold	Quenching 30 min hold		Tempering 60 min hold	
S25C	885 AC				
S35C	865 AC	865 WQ	550 WC	600 WC	650 WC
S45C	845 AC	845 WQ	550 WC	600 WC	650 WC
S55C	825 AC	825 WQ	550 WC	600 WC	650 WC
SMn438	870 AC	845 OQ	550 WC	600 WC	650 WC
SMn443	870 AC	845 OQ	550 WC	600 WC	650 WC
SCr440	870 AC	855 OQ	550 WC	600 WC	650 WC
SCM435	870 AC	855 OQ	550 WC	600 WC	650 WC
SCM440	870 AC	855 OQ	550 WC	600 WC	650 WC
SNC631	900 AC	850 OQ	550 WC	600 WC	650 WC
SNCM439	870 AC	845 OQ	580 WC	630 WC	680 WC
SNCM447	870 AC	845 OQ	580 WC	630 WC	680 WC
SUS403		975 OQ	700 WC	750 WC	
SUS430	815 AC (Annealed)				
SUS304	1080 WC (Solution treated)				

stainless steel SUS430 was annealed, and austenitic stainless steel SUS304 was solution treated, as in general usage of those materials. The other medium to high carbon steels and low alloy steels were normalized and quench-tempered, with martensitic stainless steel SUS403, as well.

Traditional materials control tests were conducted at NRIM according to the respective JIS testing methods: tests for non-metallic inclusions, hardness after quench, austenitic/ferritic grain size number, microscopic structure after heat treatments, etc.

Steels S35C, S45C, SMn438 and SMn443 were not fully transformed into martensite deep inside the materials, even after rapid water quenching, and presented partly ferritic or bainitic structures. The other quenched low alloy steels showed ordinary fine tempered-martensitic structures. No abnormality was found for 3 grades of stainless steels.

Austenitic grain size number was around 8 to 10 for all materials, except for SUS304 which revealed 4 to 5. S25C and SUS430 presented ferritic grain size number of 7 to 9 and 8 to 10, respectively. All materials more or less exhibited longitudinal fibrous structures along the rolling direction.

There microscopic aspects were taken in consideration in the analysis, but will not be discussed here except for necessary cases.

2.3 Test Procedures

2.3.1 Mechanical Properties Tests

Ordinary tensile, impact, and hardness properties were determined at NRIM according to JIS methods for every materials conditios, in order to obtain basic mechanical characteristics.

The specimen for tensile test was standard cylindrical one having 8 mm in diameter and 40 mm in gage length. Charpy test specimen was ordinary 10 mm × 10 mm rectangular bar having 2 mm deep U- or V-notches with root radius of 1.00 or 0.25 mm, respectively. Vickers hardness was measured at 196 N on Charpy specimens before the test. Figure 1 gives dimensions of the specimens.

All the tests were replicated for 3 specimens per test condition.

2.3.2 Fatigue Properties Tests

High-cycle fatigue tests were carried out under load control for the life range higher than 5×10^4 cycles. Tests were conducted by determining *S-N* curve using 18 specimens on average for each testing condition. This number of specimens was empirically chosen, assuming that at least 2 tests are needed at each of 3 to 5 stress levels to determine 'slope' part or finite life region of *S-N* curve, and around 3 more tests at least at each of 3 more levels to evaluate fatigue limit in 'horizontal' part.

All tests were conducted according to the respective

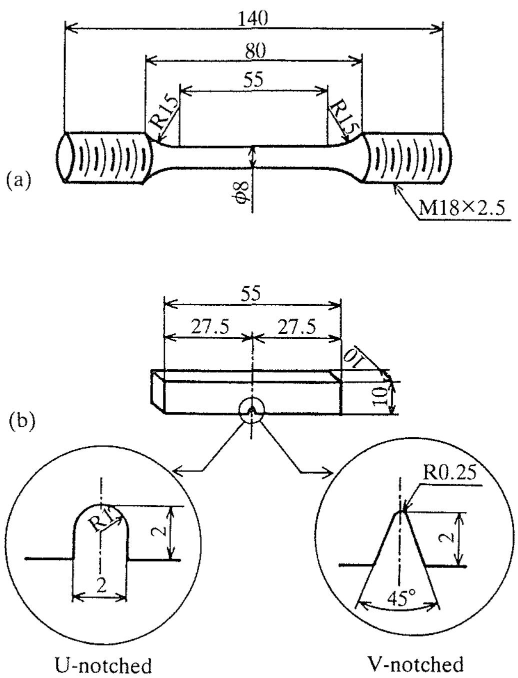

Fig. 1 Specimens for (a) tensile test and (b) Charpy impact test.

JIS/ISO, at room temperature in laboratory air, with smooth round bar specimens of different shapes depending on the testing machines. Specimens surface was carefully machined to minimize the effect of machining and finished by longitudinal polishing with 600 grade water proof silicone carbide paper. Testing machines were periodically calibrated and allocated with statistical care so as to eliminate unexpected bias in the results.

Various testing machines in the following are used, with specimens of a common test section having diameter ϕ, at indicated frequencies avoiding heating-up of specimens during tests:

- Rotating bending with ϕ 8 mm specimens: 27 sets of 4-point bending type machines at 50 Hz having capacity of 1000 N·m, and also 12 sets of cantilever bending type at 1–10 Hz and 50 N·m
- Torsional loading with ϕ 8 mm specimens: 11 sets of mechanical resonance type at 33 Hz and 50 N·m
- Axial loading with ϕ 6 mm specimens: 2 sets of electromagnetic resonance type at 120–160 Hz and 50 kN, and also 2 sets of servohydraulic type at 5–20 Hz and 50 kN

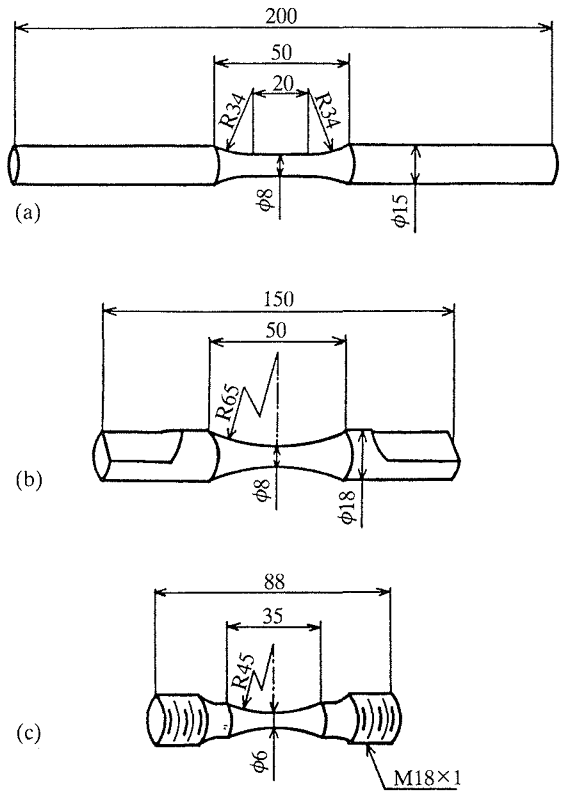

Fig. 2 Specimens for fatigue test under (a) rotating bending, (b) reversed torsion and (c) axial loading.

Figure 2 gives dimensions of the specimens. Rotating bending fatigue tests were conducted for all the materials conditions, but the orther tests were subject to typical conditions because of test capability restrictions: torsional fatigue only for materials of medium compositions, and axial fatigue for medium materials with medium heat treatments.

2.4 Data Analyses

Statistical analyses were conducted for the acquired data from various point of views. Some were to find useful correlations between different property values, some were to check occasional anomaries in the data, and some were to extract condensed property parameters from distributed data.

Ordinary statistical computations are not described here, but two original methods employed in this work will need to be explained.

2.4.1 Simultaneous Regression

In ordinary linear regression problem where a model

$$y = ax + b \tag{1}$$

is considered, x is independent variable which can be set exactly at desired values in the measurement of y. A simple example for explanation would be the weight of books for y and the number of pages for x. y is called as dependent variable and subject to statistical variation. The coefficient a can be estimated from measured data, by minimizing the sum of squared residuals in y, or on $x-y$ co-ordinates the sum of squared distances in the ordinate direction between individual data and the regressed curve.

Suppose now that the weight y is plotted against the thickness of book as x. The latter should contain statistical error, because it is also dependent on the number of pages. In this case, the error is to be considered both for y and x simultaneously, as they are equally dependent on the measurement condition.

In such a circumstance, the sum of squared distances in the perpendicular direction from the curve to each data point is to be minimized. This gives the slope of regressed curve, as in the principle component analysis, as[25)]

$$a=\sqrt{(SSY/SSX)} \tag{2}$$

where SSY and SSX are the variances of y and x, respectively. b is estimated as in the ordinary way,

$$b=(\sum y-a\sum x)/n \tag{3}$$

where n is the number of data points.

The method is widely used in analyzing the correlation between different properties of materials in this paper.

2.4.2 Analysis of *S-N* Curve

Statistical planning of fatigue tests and analysis of acquired data is in general not an easy problem.

One of the particularities of fatigue data is that it substantially involves truncated data. Fatigue test can be often suspended at prescribed number of cycles, when it is conducted at low stress levels. The data is called "truncated" in this case and gives information only that the fatigue life is longer than that number of cycles. A rough sketch of the analysis method is given here, as the detail was reported already[25,26)].

Probit analysis method is known to be applied to those suspended data. It is in fact possible to know relationship of the failure probability, p, to the stress level, S, by conducting replicated fatigue tests at several levels of S. Experimental data for p is calculated as the percentage of failed specimens at each level, observed before the predetermined number of cycles for test truncation.

In the Probit method, the sets of p-S data can be plotted on the normal probability paper to be fitted to a straight line, assuming a normal distribution for the distribution of fatigue strength. The mean of fatigue strength is then known as the intersection of the fitted line and $p=50\%$, and the standard deviation as the inverse of the slope of line. At least two or more sets of p-S observations are needed to evaluate the distribution, as the process requires determination of a straight line on the probability paper.

However, only one set of data can be enough, if the problem is to determine a straight line at a given slope. This is the case that p-S data is analyzed under given standard deviation[25)]. This method is in fact very advantageous for the analysis of ordinary small sample S-N data, as those data rarely include enough suspended data pertaining to several stress levels. The question is how to find the standard deviation of fatigue strength.

The standard deviation can be approximated by the root mean square of residuals from the fitted mean curve to the 'slope' part of S-N data. The simultaneous regression method was used to fit the slope part data, considering that the source of scatter is twofold, both in life and strength. The former is intrinsic to the fatigue process itself, and the latter is due to the assumption that a same stress cannot cause the same damage in different specimens because of materials strength variations. An experimental evidence supports this hypothesis[25)].

In the present paper, a hockey stick type bi-linear S-N curve is fitted to the data on log-log coordinates in order to determine the parameters characterizing the curve. They are: slope A, knee point N_w in cycles, fatigue limit σ_w in N/mm^2. The equation of S-N curve is then,

$$y=A\{|x-D|-(x-D)\}/2+E \tag{4}$$

where $y=\log\sigma$, $x=\log N_f$, $D=\log N_w$ and $E=\log\sigma_w$.

The S-N curve thus determined represents average high cycle fatigue property of the materials at 50% of fracture probability. Coefficient of variation CV in fatigue strength can be calculated from the sum of squared residuals from the curve. Example will be shown later in chapter 4.

It is noted that the above-explained statistical method is in principle the same as the one involved in the standard method of statistical fatigue testing[27] by Japan Society of Mechanical Engineers (JSME). However the actual analysis was not dependent on the standard, since the majority of the work was carried out before the establishment of JSME standard.

3. Reference Mechanical Properties of JIS Steels

In this chapter will be examined how the basic mechanical properties vary according to the grade of steels and following the heat treatments, and how they can be correlated to each other.

3.1 Variation of Properties Due to Heat Treatment

Figure 3 shows tensile strength data of various quench-tempered steels plotted against tempering temperature. All the data of 3 tests per materials condition are plotted here. The band in each diagram gives 95% confidence intervals of estimates obtained by ordinary regression analysis, assuming linear relations between strength and temperature for these temperature ranges, and at the same time, between scatter of strength and temperature, as well.

It is noted that the tensile strength is systematically decreasing, together with its scatter, when the tempering is conducted at higher temperatures. Similar tendency is observed for the other strength parameters, such as upper yield strength and/or 0.2% proof stress, true fracture strength and Vickers hardness[24].

The data in Fig. 1 is suggesting that the same level of strength could be attained with different grades of steels by selecting appropriate tempering temperatures, while the scatter within the steel grade would not be the same.

Figure 4 demonstrates reverse dependence on tempering temperature for elongation, where the value is increasing with increasing temperaure. The tendency is the same for the other ductility parameters, such as uniform elongation and reduction in area. Charpy impact values at room temperature vary in the same way, proving that they are oftern referred as an index of ductility in practice. The work hardening exponent behaves similarly to ductility parameters, as it has been said to represent the elongation at maximum load on true stress-strain diagram.

The systematic change in strength and ductility

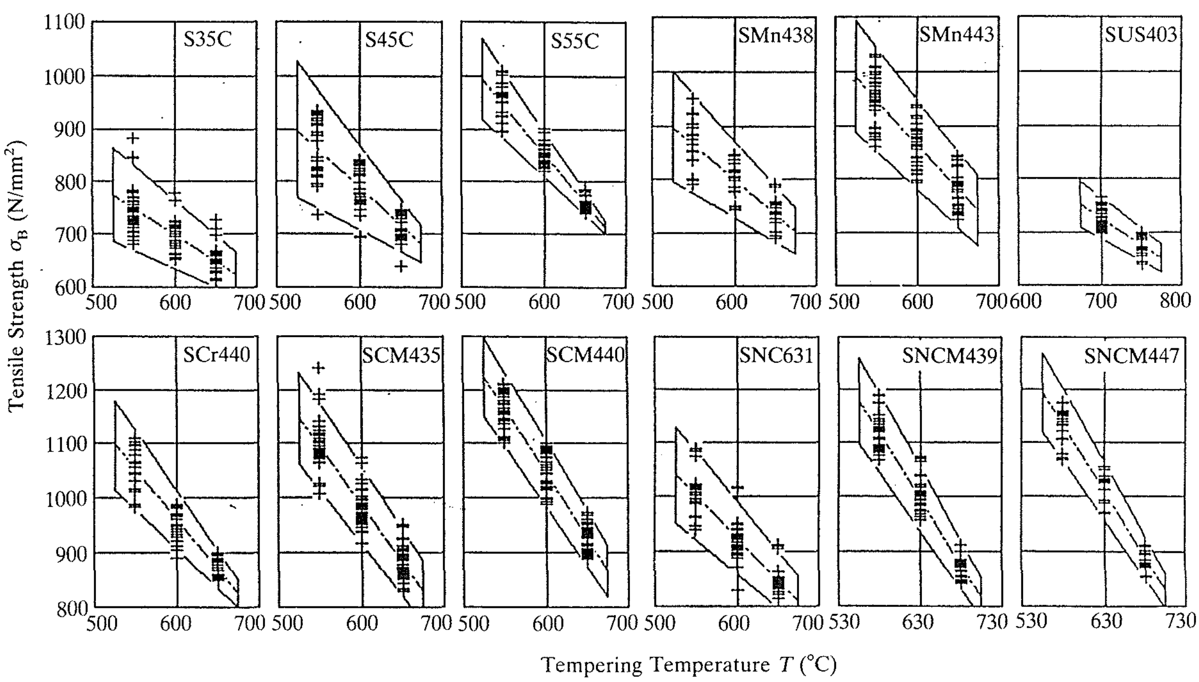

Fig. 3 Relation of tensile strength σ_B and tempering temperature T.

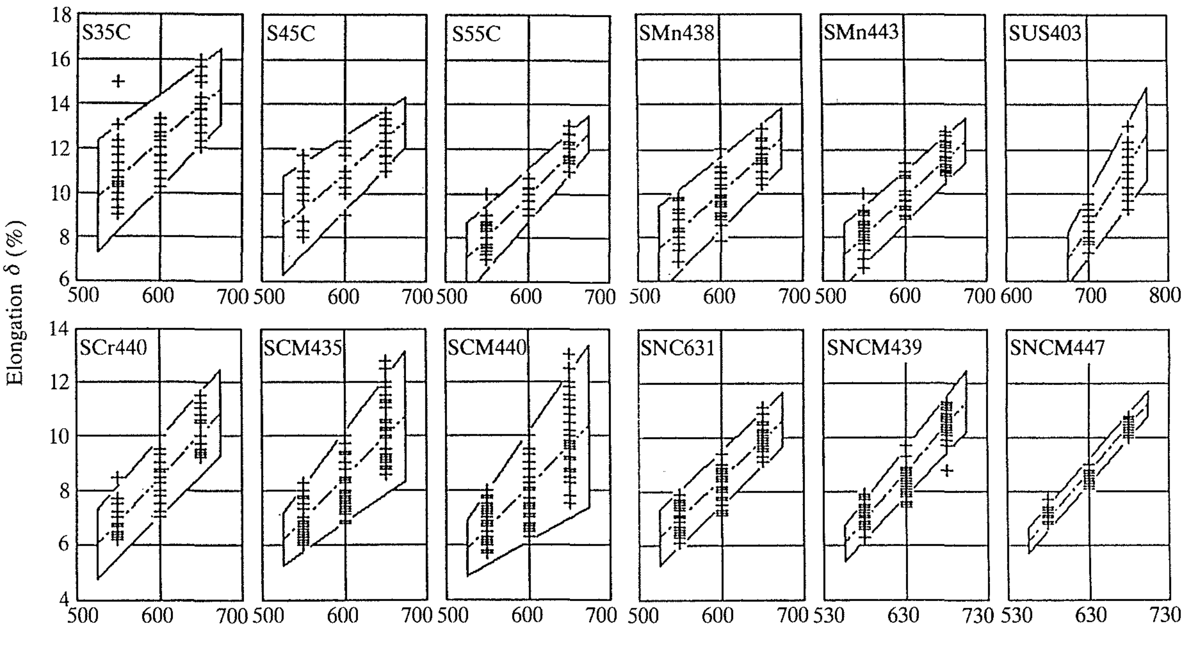

Fig. 4 Relation of elongation δ and tempering temperature T.

parameters with tempering is considered to be related to the quench hardenability of steels. In fact, addition of the alloying elements such as Mn, Cr and Ni increase the hardness after quench with varying degrees with their amount. In other words, it increases the strength parameters and decreases the ductility parameters. This hardening effect is weakened by tempering with greater extent when the tempering is performed at higher temperatures, resulting the decrease in scatter between steels.

It can also be seen in Fig. 4 that the change in scatter of elongation associated with tempering temperature is not unique for different steels. It decreases as temperature increases for general cases, but increases obviously for steels SCM435 and SCM440, in contrast to the others. However, the reduction in area for the same steels revealed decreasing scatters with increasing temperature, as in general steels[24].

The increasing scatter with enhanced tempering, observed for the elongation of SCM steels, can not be explained by the general trend of quench-tempering. Similar abnormal trend was found also for true fracture strength and Charpy V-notch impact value for the same SCM steels. It will need further study to understand the cause of this trend, which can seemingly be related to the instability at fracture for that type of steels.

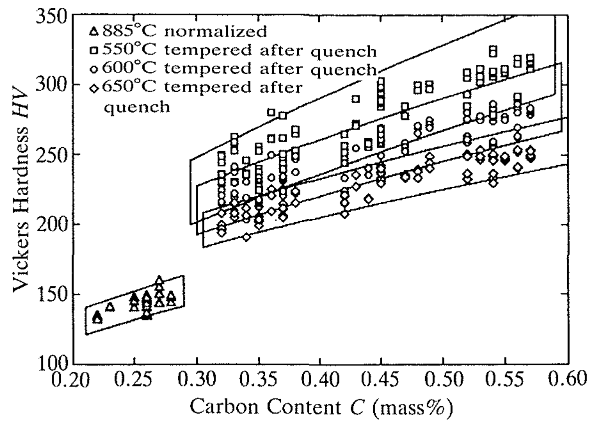

Fig. 5 Typical variation in Vickers hardness HV for carbon steels in function of carbon content C and heat treatments.

Figure 5 shows typical dependence of Vickers hardness, HV, on their carbon content, $C\%$, for carbon steels. The 95% confidence bands in the figure were traced after regression analysis, assuming a mathematical relation for quench-tempered steels,

$$\log(HV) = a \log(C) - b \log(273+T) + c \quad (5)$$

where T is tempering temperature and a, b and c are constants.

It would be self-understanding that the hardness is increasing with carbon contents for quench-tempered steels, as the quench hardenability is directly related to the carbon contents. Hardness is also increasing for normalized steels, as the amount of pearlitic structure is increasing with carbon contents. The figure allows to estimate the hardness range of other classes of steels not tested in the program, such as S43C or S48C steels, having 0.40–0.46C and 0.45–0.51C, respectively.

Quite similar results were obtained for the other strength parameters as yield and tensile strengths and contrary results for the ductility parameters as elongation and reduction in area[24].

A detailed list of statistically analyzed results will be found in Appendix.

3.2 Correlation Between Mechanical Properties

It is empirically known that good correlation is often found between different mechanical properties of metallic materials, as for example the one between tensile strength and hardness. In some circumstances, the mechanical property is said to be estimated satisfactorily in an engineering sense from basic materials parameters such as hardness. Actual situation is shown in the following.

3.2.1 Monotonic Strength Parameters

Mechanical properties tested by a single application of load are oftern called 'monotonic' properties to distinguish them from 'cyclic' ones obtained under repeated loading characterizing fatigue.

There are 5 monotonic strength parameters deduced from the test, namely, upper yield strength, 0.2% proof stress, tensile strength, true fracture strength, and Vickers hardness. Statistical analyses were carried out to find significant correlations between them, and some typical ones will be displayed in the following figures.

In each figure the 95% confidence bands are shown for of estimates obtained by the simultaneous regression method explained above. The analysis was conducted on log-log coordinates by changing the materials grouping and the results presenting maximum coverage was shown in the figure.

Figure 6 shows typical dependence of 0.2% proof stress on tensile strength. It is interesting to note that

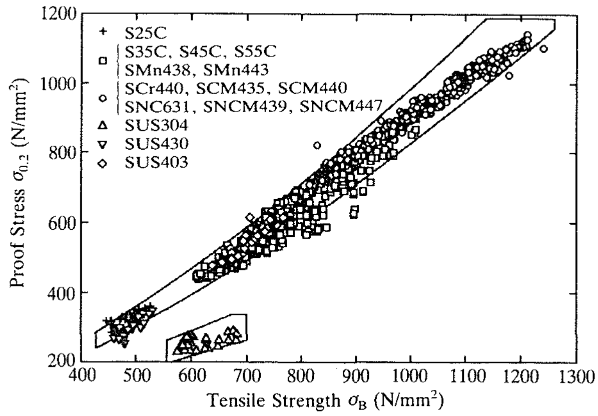

Fig. 6 Relation of 0.2% proof stress $\sigma_{0.2}$ to tensile strength σ_B.

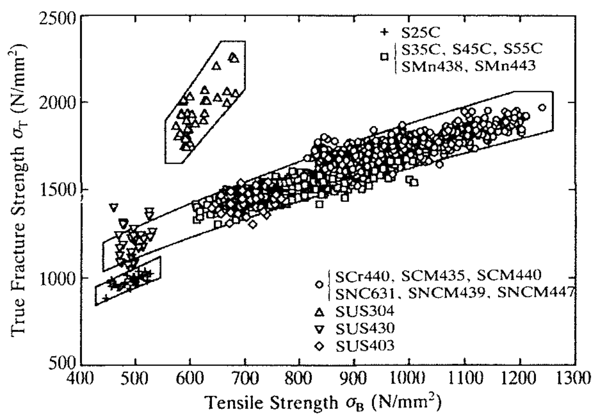

Fig. 7 Relation of true fracture strength σ_T to tensile strength σ_B.

many quench-tempered carbon and low alloy steels behave quite similarly, together with 13Cr stainless steels SUS403, as they all have high-temperature tempered martensitic (HTTM) structures. Another grouping is possible for normalized low carbon steels S25C having ferrite-pearlite (F/P) structures and annealed 17Cr stainless steels SUS430 having ferritic structures, Fig. 6, while they are tentatively incorporated in the HTTM group. The third group is solution treated 18Cr-8Ni stainless steels SUS304 with austenitic structures.

Figures 7 and 8 reveal similar dependence of other monotonic properties on tensile strength. True fracture strength in Fig. 7 is considered to be the limiting property of the matrix at severely deformed state, whereas Vickers hardness in Fig. 8 reflects the resistance of matrix at local deformation. HTTM

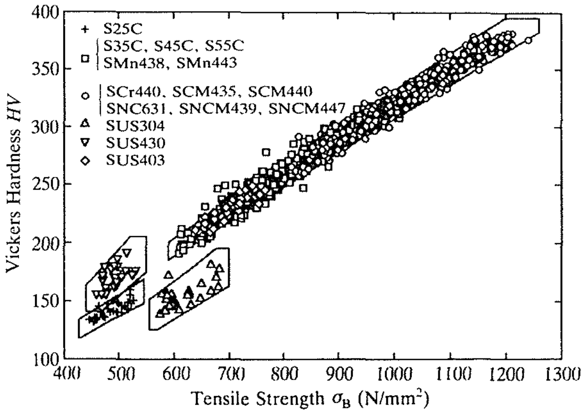

Fig. 8 Relation of Vickers hardness HV to tensile strength σ_B.

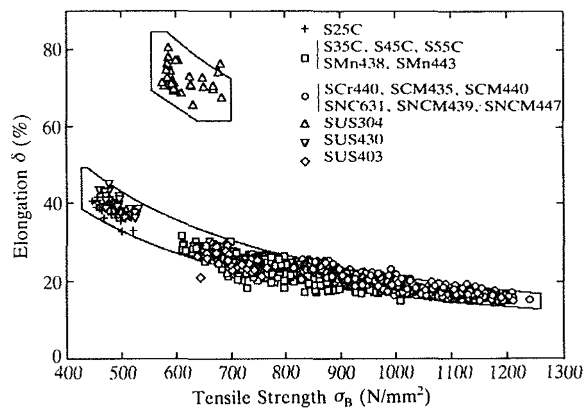

Fig. 10 Relation of elongation δ to tensile strength σ_B.

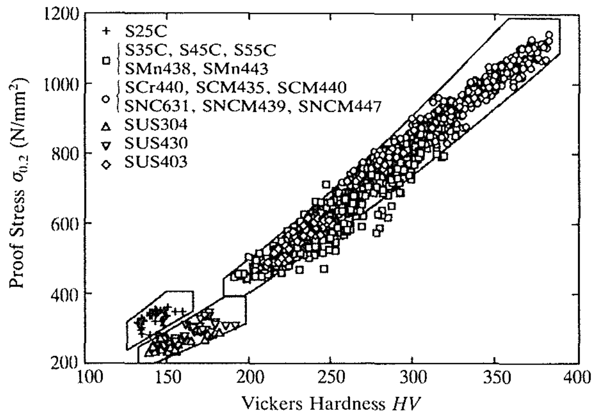

Fig. 9 Relation of 0.2% proof stress $\sigma_{0.2}$ to Vickers hardness HV.

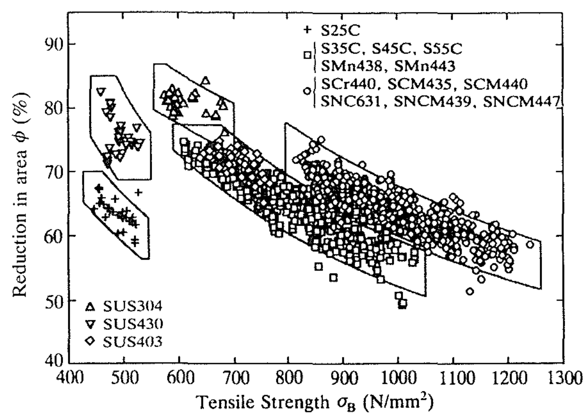

Fig. 11 Relation of reduction in area ϕ to tensile strength σ_B.

materials behave always in one group, but the grouping of F/P materials is not unique. The behavior of F/P materials seems to be dependent on the amount of plastic deformation which is brought about when the property in question is measured.

In Fig. 9 where proof stress and Vickers hardness are correlated, the group F/P is closer to the other groups, the reason being assumed that the two properties are determined both at relatively small plastic strains.

For austenitic stainless steels the behavior is believed to be more deformation sensitive than F/P steels. They are characterized with the lowest proof stresses and the highest true fracture strengths for materials of same strength levels, as can be seen in Figs. 7 and 8, implying their pronounced work hardenability.

The ratio of tensile strength in N/mm^2 to Vickers hardness, σ_B/HV, is determined for the present data, as

- Ferritic stainless steels, SUS430: 2.91
- HTTM carbon and low alloy steels: 3.12
- Low carbon F/P steels, S25C: 3.44
- Austenitic stainless steels, SUS304: 4.00

3.2.2 Monotonic Ductility Parameters

Figures 10 to 12 show typical monotonic ductility parameters obtained from tensile test. They are all decreasing with increasing strength, but in various ways from case to case.

The relationship between elongation and tensile strength, Fig. 10, seems to be unique for different microstructural groups of steels, except for austenitic steels. However, the grouping becomes far complex when reduction in area is plotted against tensile

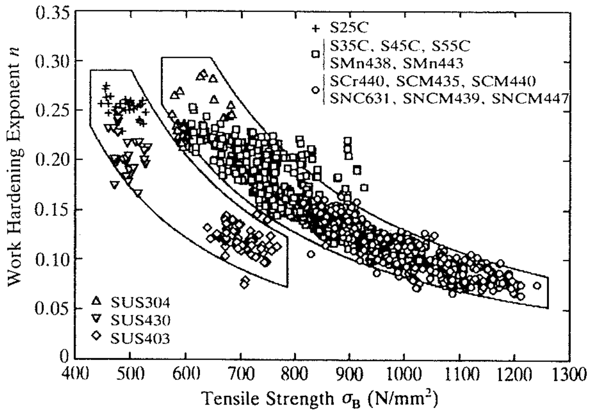

Fig. 12 Relation of work hardening exponent n to tensile strength σ_B.

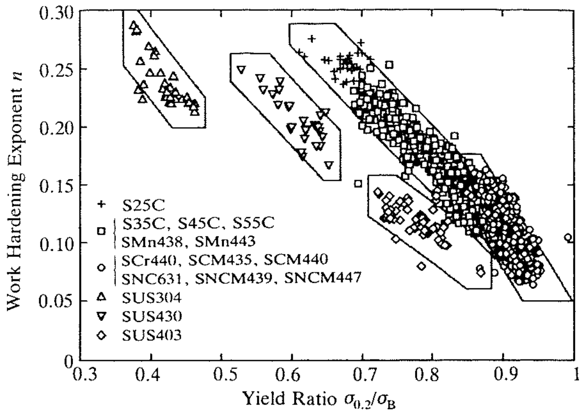

Fig. 14 Relation of work hardening exponent n to yield ratio $\sigma_{0.2}/\sigma_B$.

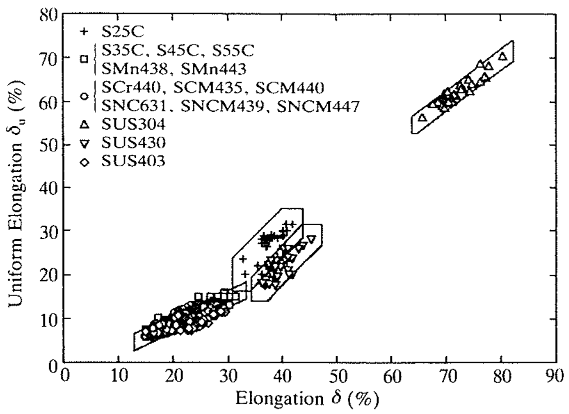

Fig. 13 Relation of uniform elongation δ_u to elongation δ.

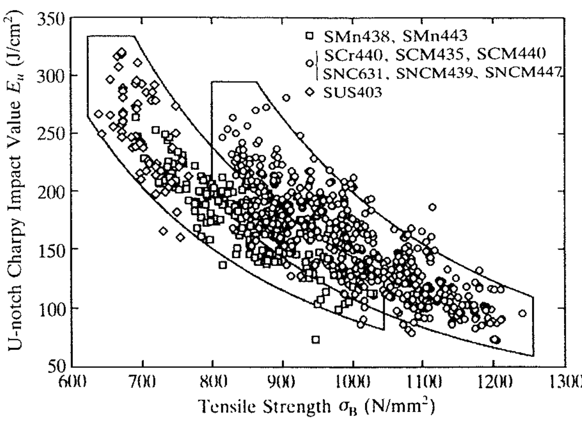

Fig. 15 Relation of U-notch Charpy impact value E_U to tensile strength σ_B.

strength, Fig. 11. Even within HTTM structures, carbon and low-alloy steels do not behave in the same way.

It is considered that the correlation between properties is in principle different for different microstructures for those highly deformed ranges. On the contrary, the work hardening exponent which was deduced for plastic deformations ranges of 2–5% for HTTM steels and 4–10% for the others, Fig. 12, shows no clear discrepancy within HTTM steels.

Figure 13 shows the relation of uniform elongation between total elongation. It suggests different deformation stabilities of microstructures against necking. Austenitic steels show the highest stability here, as the ratio of uniform to conventional elongations is near 0.9, HTTM carbon and low alloy steels the lowest with the ratio less than 0.5, and ferritic steels between the two.

Figure 14 correlates work hardening exponent of different groups of steels with yield ratio. This can be understood that the relative stress increment from yield to ultimate tensile strengths, $(\sigma_B-\sigma_{0.2})/\sigma_B$, is more directly related to the work hardening. It is observed only in this figure that martensitic stainless steels SUS403 show different response from the other HTTM steels.

Figure 15 represents relation of Charpy impact values to tensile strength for HTTM low alloy steels. U-notched specimens are generally used in JIS for low alloy steels, while for carbon steels are specified only with V-notched specimens. The results for HTTM carbon steels are not represented here but quite similar to those in Fig. 15.

There is no substantial difference between the

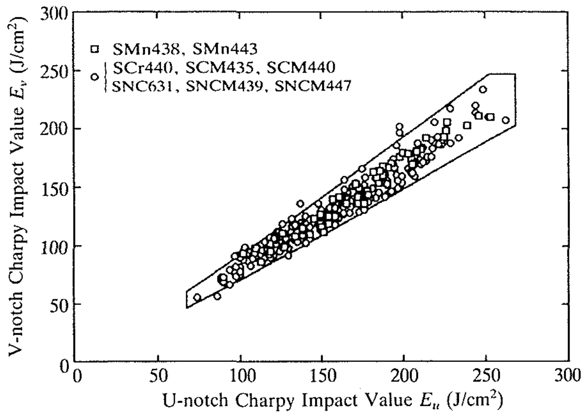

Fig. 16 Relation of V-notch Charpy impact value E_V to that of U-notch E_U.

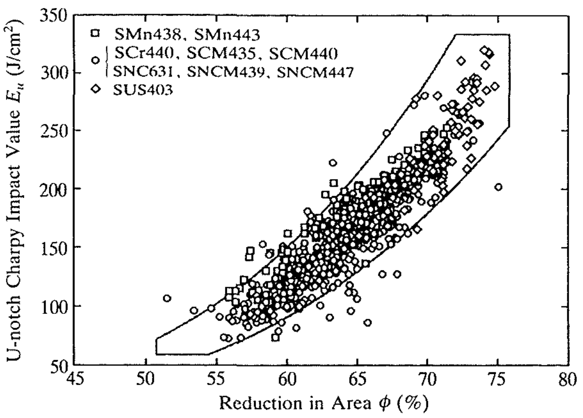

Fig. 17 Relation of U-notch Charpy impact value E_U to reduction in area ϕ.

results with U-notched specimens and V-notched, excepting that the former give 1.2 times larger values, as can be seen in Fig. 16.

Figure 17 shows that the Charpy impact value at room temperature can be directly correlated to the reduction in area, independent to the classes of HTTM steels. This explains why the impact value is often referred to evaluate monotonic ductility of the engineering materials.

4. Reference Fatigue Properties of JIS Steels

Figure 18 shows an example of S-N data obtained for SCM440 steels tempered at 600°C after normalizing and quenching. Curves represent, from lower to upper, responses at 10, 50 and 90% of failure probabilities, respectively, obtained after the analysis by the bi-linear curve fitting explained above. There

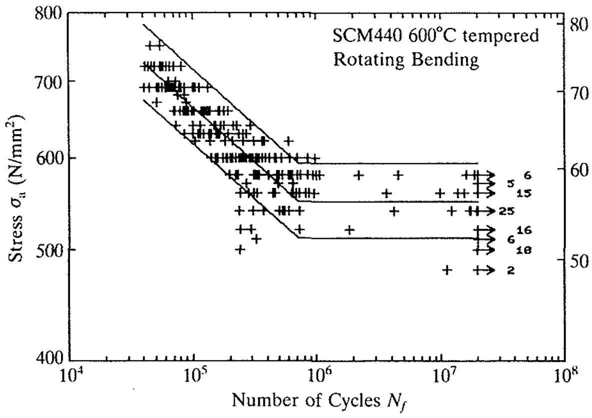

Fig. 18 Typical S-N diagram showing rotating bending fatigue properties of SCM440 steel tempered at 600°C after quench. Numbers in the figure indicate those of runout speciments at the test stress level.

are in total 303 data points pertaining to 15 different heats, which are collectively analyzed in this case.

Analysis was of course made for each set of individual heat, but the results are not given here. There have been found some interesting statistical trends, such as the slope of S-N curve increases and the knee point decreases, with increasing materials strength. Details can be found in a separate report[25], and are not described here.

A full list of analyzed data will be given in Appendix for information. It gives S-N curve parameters for each grade of steels under different load conditions. S-N curves are analysed for the plot on ordinary stress scale and for normalized stress scales both by tensile strength and Vickers hardness as well.

4.1 Variation of Fatigue Strength due to Heat Treatment

Figure 19 shows the variation of fatigue properties under rotating bending determined at each materials conditions in this work. The results for S25C and SUS304 are not given here and can be found in Appendix. As far as the fatigue limit is concerned, it revealed very similar dependence on tempering temperature to the monotonic strength parameters shown earlier: it was decreasing with its scatter with increasing temperature.

The dependence on tempering temperature was generally the same for fatigue strengths under torsional and axial loading. They were also found to be correlated to the carbon content in the same way as

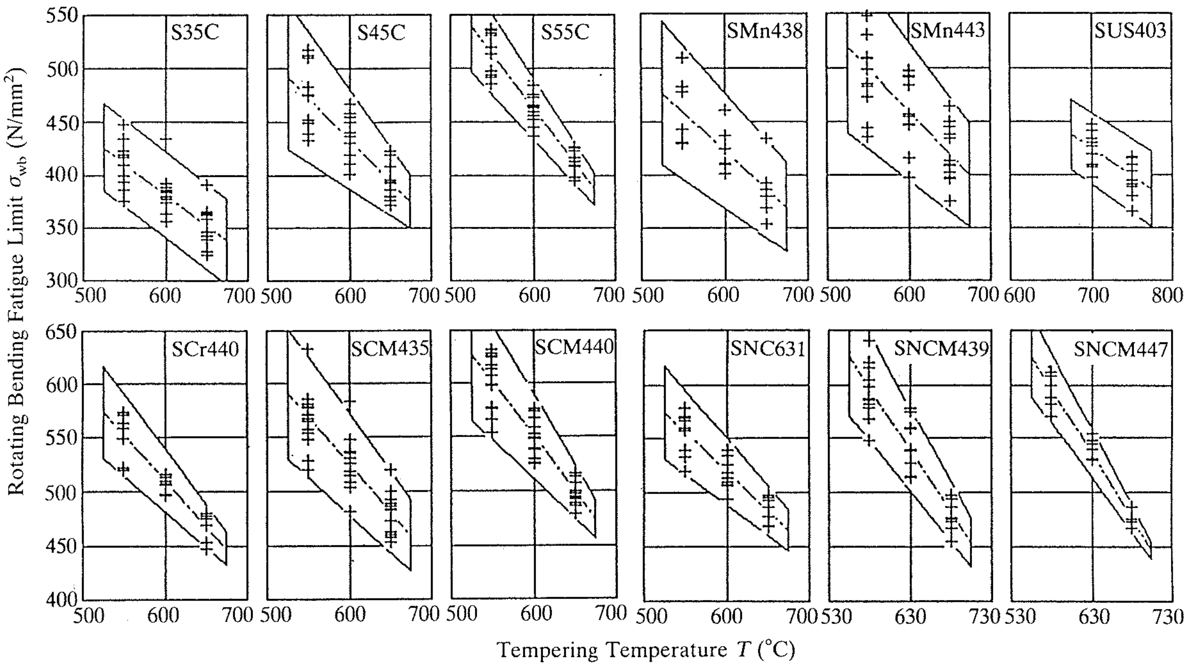

Fig. 19 Relation of fatigue limit under rotating bending σ_{wb} and tempering temperature T.

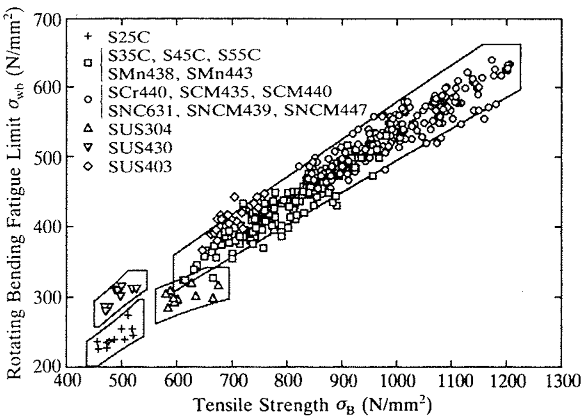

Fig. 20 Relation of fatigue limit under rotating bending σ_{wb} to tensile strength σ_B.

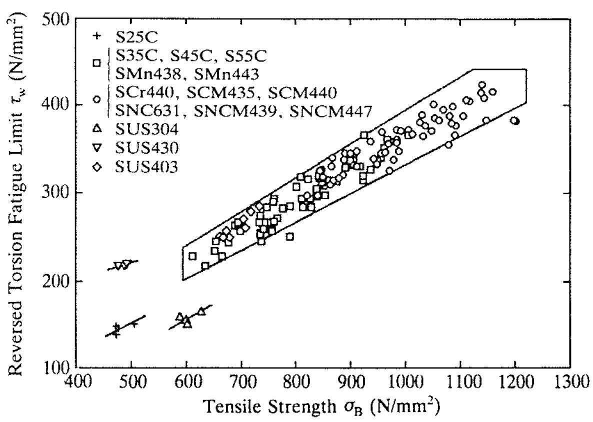

Fig. 21 Relation of fatigue limit under reversed torsion τ_w to tensile strength σ_B.

shown in Fig. 5. It can be concluded that the fatigue strength behave substantially in the similar way to the monotonic strength parameters.

4.2 Correlation Between Fatigue Strength and Mechanical Properties

Typical correlation of fatigue strength to mechanical properties can be found in the following.

Figure 20 shows the relation of fatigue limit under rotating bending to tensile strength of all the materials tested. There is clear dependence on the microstructures: HTTM carbon and low alloy steels are all in a band where mean coefficient of proportionality is 0.542 with standard deviation of 0.0233. S25C steels with F/P structure and SUS304 at austenitic structure are placed at the bottom, with the mean coefficient of 0.496 and 0.492, respectively, and ferritic SUS430 steels at the highest, with 0.611.

Similar relations are obtained for fatigue limits under reversed torsion, Fig. 21, and under axial loading at reversed tension-compression and at repeated tension, Figs. 22 and 23, respectively. The range of scatter was not shown in these figures except for

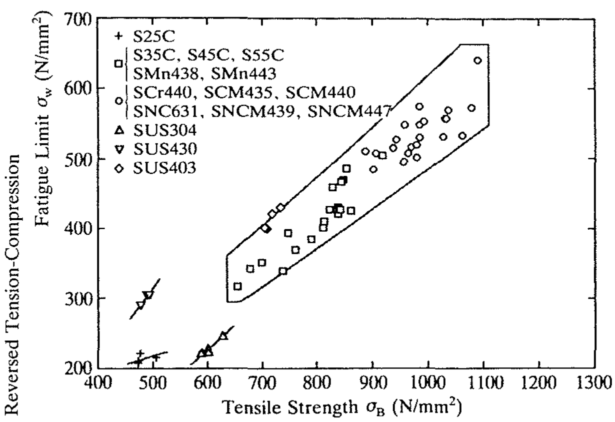

Fig. 22 Relation of fatigue limit under reversed tension-compression σ_w to tensile strength σ_B.

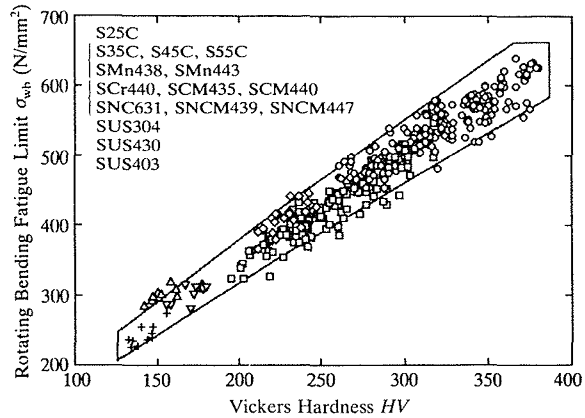

Fig. 24 Relation of fatigue limit under rotating bending σ_{wb} to Vickers hardness HV.

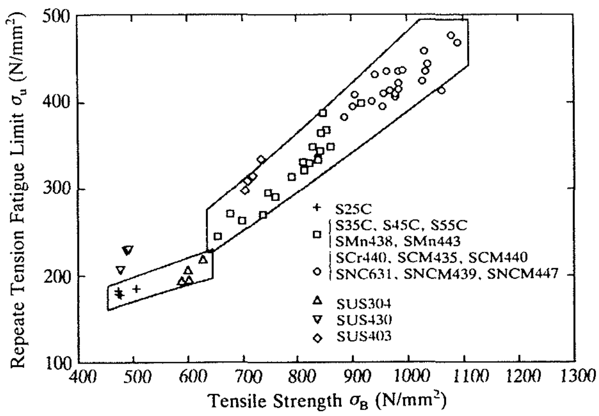

Fig. 23 Relation of fatigue limit under repeated tension σ_u to tensile strength σ_B.

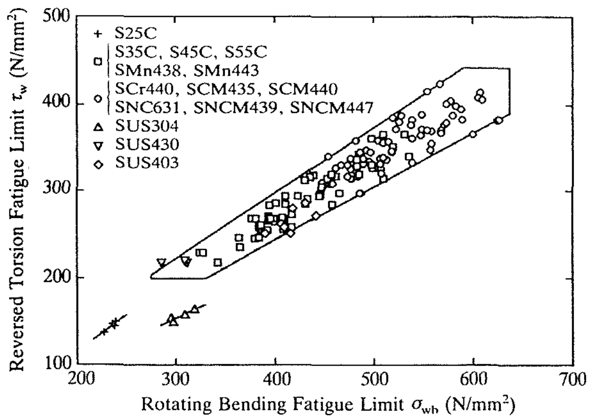

Fig. 25 Relation of fatigue limit under reversed torsion τ_w to fatigue limit under rotating bending σ_{wb}.

HTTM materials, as the number of test was too small for the others. The relation is always in the same tendency as seen in Fig. 20, suggesting systematic relations between fatigue strengths under different loading conditions.

The results shown above imply that the fatigue limit can be predicted from tensile strength of the materials. It should be noted however that the tensile strength given in ordinary mill sheet is not to be simply used for the prediction. The mill sheet reports generally the chemical composition and typical mechanical properties on test coupons, whose size and heat treatment conditions may not be the same as those for the actual situation.

Figure 24 gives the relation of fatigue limit under rotating bending and Vickers hardness. The correlation is excellent in this case, with negligible difference between materials group of different microstructures. Following mathematical expression can be used,

$$\log(\sigma_{wb})=0.923\log(HV)+0.417\pm0.0197 \quad (6)$$

where the value after the compound sign is standard error. This error corresponds to the coefficient of variation of 4.54% in σ_{wb}, telling that the 95% confidence interval for the estimate is 8.9% for all materials in this case.

Similar relation is found for the other fatigue strengths, but with some dependence on microstructures. In case of HTTM steels, the following ratios to HV may be used for rough estimation of fatigue strengths:

- for rotating bending: 1.69
- for reversed torsion: 1.13
- for reversed tension-compression: 1.66

Fatigue strengths under reversed torsion and re-

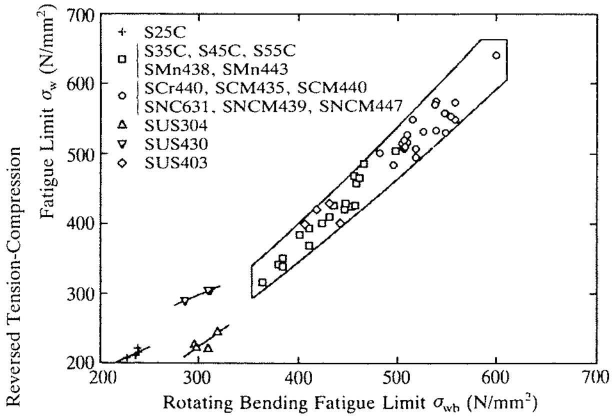

Fig. 26 Relation of fatigue limit under reversed tension-compression σ_w to fatigue limit under rotating bending σ_{wb}.

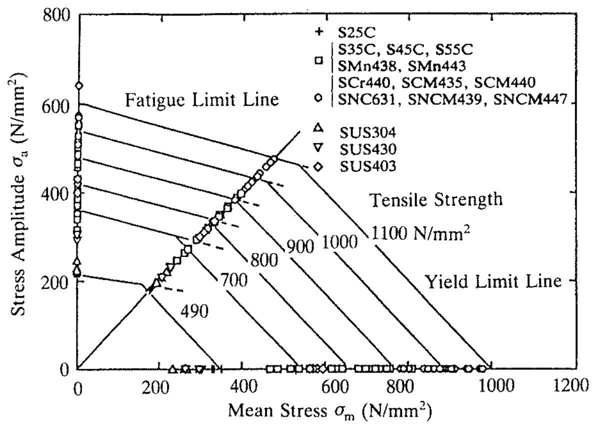

Fig. 28 Fatigue limit diagram relating amplitude σ_a and mean σ_m of materials at different tensile strength levels.

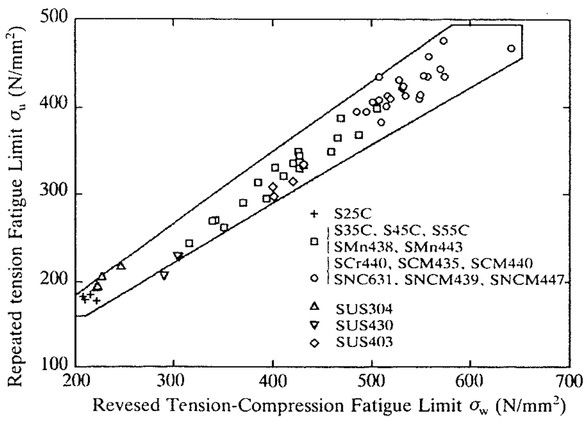

Fig. 27 Relation of fatigue limit under repeated tension σ_u to fatigue limit under reversed tension-compression σ_w.

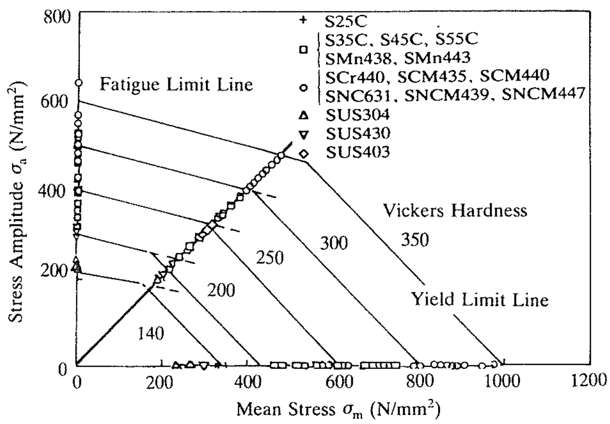

Fig. 29 Fatigue limit diagram relating amplitude σ_a and mean σ_m of materials at different hardness levels.

versed tension-compression are plotted in Figs. 25 and 26, respectively, against rotating bending fatigue strength. Here again the behabior is slightly different for steels with different microstructures.

Figure 27 gives the relation between fatigure strengths under repeated tension and under reversed tension-compression. A general ratio of 0.78 is found for HTTM steels of higher strengths, while it is variable for steels of lower strengths and higher ductilities.

The same data is expressed as Haigh's diagram, Fig. 28, in relation of amplitude to mean stress of fatigue limit for different strength levels of steels. In this diagram, fatigue limit lines are combined to yield limit lines, indicating that the materials can be used without failure in zones under each curve. The lowest curve labeled 490 N/mm^2 in tensile strength represents the trend for S25C steels.

Figure 29 is again the same data but expressed for different hardness levels of steels.

The slope of fatigue limit lines for HTTM steels is 0.267 on average.

It is to note here that the austenitic stainless steel SUS304 can be heated-up when cyclically loaded at high frequencies. The fatigue data refered above was obtained at enough low cyclic rates to keep specimens at room temperature[28].

4.3 Cyclic Parameters

In parallel to the high-cycle fatigue tests for FDS program, strain-controled low-cycle fatigue property was investigated for some materials conditions[29]. The results were not included in the referred FDS, as the

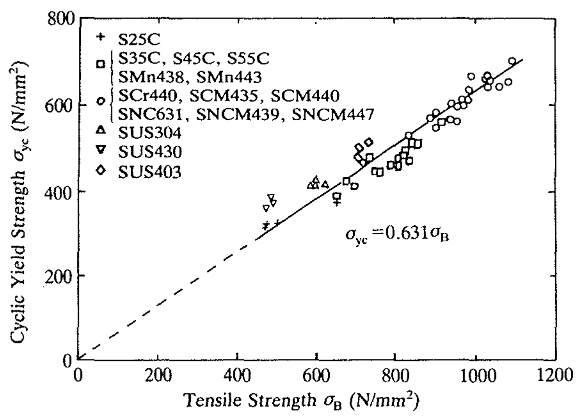

Fig. 30 Relation of cyclic yield strength σ_{yc} to tensile strength σ_B.

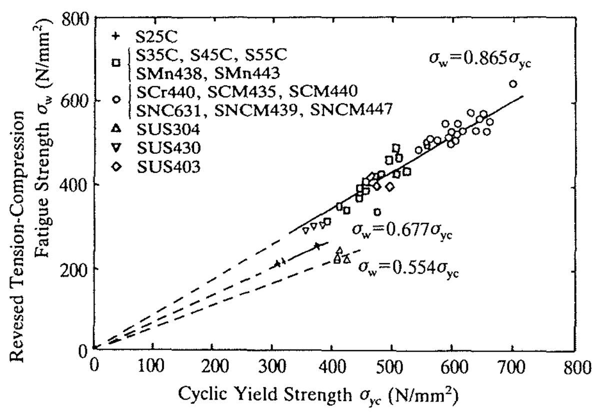

Fig. 31 Relation of fatigue limit under reversed tension-compression σ_w to cyclic yield strength σ_{yc}.

work was conducted in view of obtaining preliminary data for the succeeding series of FDS program. More comprehensive data can be found in other FDS publication[17)–22)], which will be subject to another FDS Technical Documents in preparation.

It is already known that the cyclic stress-strain relationship in low-cycle regime is of substantial importance to characterize fatigue of materials. In fact, well-annealed materials is easy to be deformed, as the dislocation density is low in the matrix. By the application of cyclic strains, the density is increased in matrix and stabilized at a state reflecting the range of strains. The materials is then cyclically hardened to a degree characteristic to the dislocation structures.

On the contrary, application of cyclic strains can decrease the dislocation density, when it was initially at very high stages as in quenched or severely cold-worked materials. The materials is then cyclically softened. The stable densities of dislocations in both cases are characteristic to the strain range, and particularly to the metallurgical structure of materials. The stress-strain relationship of cyclically stabilized materials is therefore a key property reflecting the dislocation mobility in matrix, and thus the fatigue behavior of the materials.

Stress-strain response of cyclically stabilized materials is determined by the incremental step test in the present paper. Mateials, experimental conditions and analyzed results are reported in an earlier paper[29)]. Here will be discussed only about the relationship between fatigue strength and cyclic yield strength, σ_{yc}, defined as 0.2% offset stress on the stress-strain curve at cyclically stabilized state.

Figure 30 shows first the relation of cyclic yield strength to tensile strength of test materials. Cyclic yield was determined only for materials conditions where axial fatigue properties were investigated. As seen in the figure, there is a proportional relation between the two as a whole. In closer view, however, the coefficient of proportionality is somewhat higher for three stainless steels, *ie.* ferritic SUS430, austenitic SUS304, and martensitic SUS403, than the other HTTM carbon and low alloy steels.

Figure 31 compares axial fatigue limit under reversed tension-compression and cyclic yield strength. It is to note that the fatigue limit is systematically lower than the cyclic yield strength with varying degrees for different microstructural groups of steels. In this case, different proportionalities are distinguished, as indicated in the figure. The ratio σ_w/σ_{yc} is

- for HTTM steels: 0.86
- F/P steels: 0.68
- austenitic steels: 0.55

In conclusion, the two intrinsic characteristics, that the cyclic yield strength is dependent on the monotonic tensile strength, and that the fatigue strength is determined by the cyclic yield strength, are considered to be the cause of many correlations between different monotonic and cyclic properties.

5. Factors Affecting Fatigue Properties

Here will be discussed two important factors which often definitively affect fatigue properties of materials. One is the chemical composition governing the hardness after quench, and therefore defining mechanical properties of HTTM sttels. The other is the presence of non-metallic inclusions in the matrix which provides the initiation site of fatigue cracks through stress concentration effect.

5.1 Quench Hardenability of Steels

The hardness of a steel after quench is basically defined by its chemical composition. Higher contents of carbon, chromium, nickel, etc., are favorable for quench hardening. It is also definitively affected by the cooling rate at the quench. More the cooling rate is fast, more the hardening is effective, in general. The core part of thick materials is often found to be not perfectly hardened even by rapid cooling. This is known as the mass effect in quenching.

The quench hardenability can be expressed by an index D_I called ideal critical diameter. It is an imaginary size of cylindrical specimen, having length at 4 times of its diameter, presenting a core structure with 50% martensite by an ideal quenching at enough high cooling rate at materials surface. The ideal critical diameter is one of the parameters intrinsic to the materials quality and independent of its size and quenching conditions.

Ideal critical diameter of low alloy steels can be predicted in general by the primary austenite grain size number GS, carbon content C, and hardenability coefficient $f_{(\cdot)}$ of each element in the steel. Note that the term low alloy steel is used for steels with 5% maximum of total alloying elements. Following expression is used in this paper:

$$D_I = D_{IB} \cdot f_{Si} \cdot f_{Mn} \cdot f_{Cr} \cdot f_{Mo} \cdot f_{Ni} \text{ (mm)} \quad (7)$$

$$D_{IB} = (12.94 - 0.622 \cdot \mathrm{GS}) \sqrt{\mathrm{C}}$$

$$f_{Si} = 1 + 0.699 \text{ Si}, \quad \mathrm{Si} \leqq 0.40$$

$$f_{Mn} = 1 + 3.344 \text{ Mn}, \quad 0.60 \leqq \mathrm{Mn} \leqq 0.90$$

$$f_{Cr} = 1 + 2.160 \text{ Cr}, \quad \mathrm{Cr} \leqq 1.30$$

$$f_{Mo} = 1 + 3.014 \text{ Mo}, \quad 0.15 \leqq \mathrm{Mo} \leqq 0.35$$

$$f_{Ni} = 1 + 0.364 \text{ Ni}, \quad \mathrm{Ni} \leqq 2.80$$

where the amount of alloying element is evaluated in mass %. Factors in each equation of the hardenability coefficient are derived by least squares fitting of data in the table A3 of ASTM A255 standard[30].

Table 4 compares typical values of the ideal critical diameter for the grades of steels investigated. Grain size number GS is assumed constant for simplicity and set as GS=8. It is clear that the carbon steels are far inferior to the other low alloy steels, while SNCM steels are superior, in the ideal critical diameter. It is to note that this table gives only an information to understand general trend of quench hardenability for different steels and does not provide quantitative index allowing to predict their hardness.

Figure 32 shows, as an example, the actual situation for three grades of steels in the present work. It shows Vickers hardness distributions of steels after quench determined along an axis perpendicular to and at mid-length of the cylindrical bar stock of 200 mm long. Carbon steel S35C and Cr-Mo steel SCM 435 reveal a same high hardness at the surface, as they have same carbon content of 0.35%, but present

Table 4. Ideal Critical Diameter for Low Alloy Steels Tested

Steel	Typical composition	D_I (mm)
S25C	0.25C	4
S35C	0.35C	5
S45C	0.45C	5
S55C	0.55C	6
SMn438	0.38C-1.5Mn	35
SMn443	0.43C-1.5Mn	37
SCr440	0.40C-1Cr	72
SCM435	0.35C-1Cr-0.2Mo	98
SCM440	0.40C-1Cr-0.2Mo	110
SNC631	0.31C-2.7Ni-0.8Cr	78
SNCM439	0.39C-1.8Ni-0.8Cr-0.2Mo	150
SNCM447	0.47C-1.8Ni-0.8Cr-0.2Mo	165

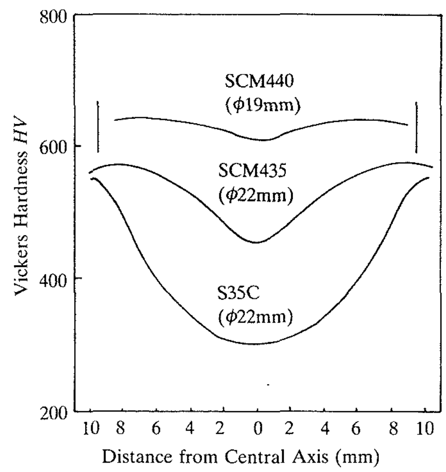

Fig. 32 Typical hardness distributions after quench.

different lower hardness values near the center according to their ideal critical diameters. Another steel SCM440, containing 0.40% of carbon, gives a higher and flat hardness distribution, proving its higher carbon content and therefore larger ideal critical diameter.

The different hardness after quench is in general inherited after tempering, and thus causes difference in mechanical properties. In the present work, the grain size was not greatly different between test materials regardless of steel grades and heats/lots from different companies, as described earlier in 2.2. The heat-to-heat variation of quench hardenability was found dependent almost on the variation in the content of carbon and other alloying elements.

It would not become possible, however, to predict final mechanical properties only from the chemical composition, because there are still many other influencing factors, such as size and surface conditions which also affect the cooling rate. The problem is particularly complex for the fatigue performance, which could definitely be changed by the presence of non-metallic inclusions, as described next.

5.2 Effect of Non-Metallic Inclusions

As shown earlier in 4.2, fatigue strength increases in general with increasing monotonic strength, in approximately proportional way. However, by more careful observation, the scatter of fatigue strength at given monotonic strength is found to be asymmetric, as can be seen for example in the relation of fatigue limit to hardness, Fig. 24. There are more data lying lower outside of the confidence band. The reason for this occasional drop in fatigue strength of some heats/lots is explained by the harmful effect of non-metallic inclusions.

In fact, special steels as investigated in this FDS program contain generally small amount of non-metallic inclusions. Type, size and quantity of non-metallic inclusions are variable according to the steel making process and steel grades. The presence of inclusions is in principle harmful especially for high-cycle fatigue performance, as they can be the initiation source of fatigue cracks through their stress concentration effect.

Photo 1 is a typical example of fatigue crack initiated at a non-metallic inclusion. It shows the fracture surface of rotating bending fatigue specimen of SMn438 steel tested at 400 N/mm^2 and failed at 3.46×10^5 cycles. On low magnification view at the left, radial lines-like feature tells that the fracture initiated from a defect at the top surface of the specimen; at high magnification on the right, this defect is found to be a globular composite of non-metallic inclusions.

For carbon and low alloy steels tested in this program, the non-metallic inclusions found at the origin of fatigue fracture are found normally as the globular mixture of oxides of Al, Si and Ca, and other compounds such as MnS. These elements are considered to have come into the steel during steel making process, as they are used as de-oxidation agents or for refractory materials.

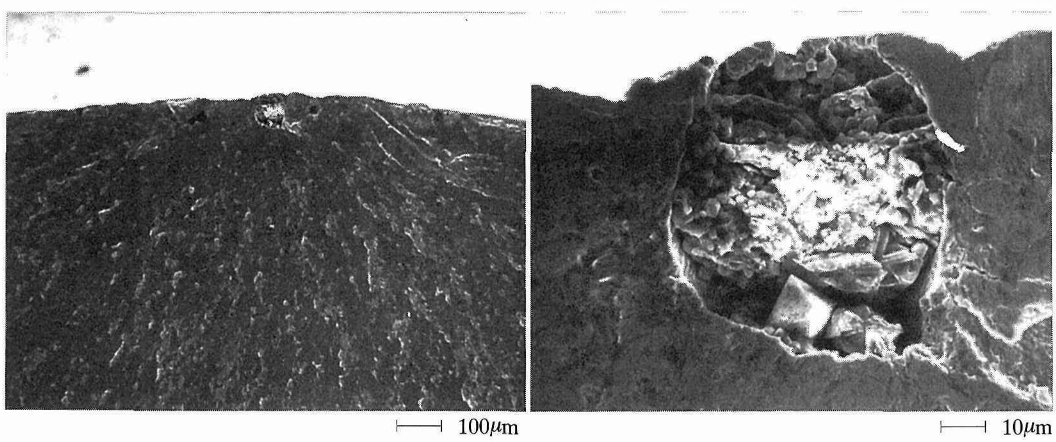

Photo. 1 Typical fractography showing non-metallic inclusion at fatigue crack initiation site.

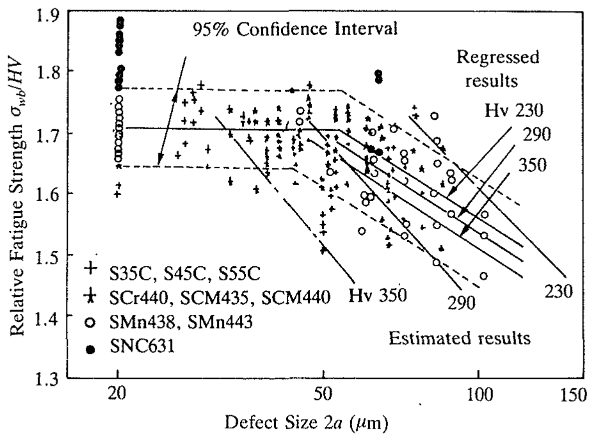

Fig. 33 Relation of relative fatigue strength and size of non-metallic inclusions at fatigue crack initiation site.

In any case, it is empirically known that the relative fatigue strength is decreasing with increasing size and number of these non-metallic particles. In view of finding quantitative information, an extensive SEM analysis was conducted on the failed specimens of various steel grades tested at low stress levels under rotating bending.

Figure 33 shows the results by plotting relative fatigue strength to Vickers hardness against defect size[31]. Here the defect size is evaluated by averaging the largest three diameters of non-metallic inclusions found for a given heat/lot of steel resgardless of tempering temperatures. This is because the size of inclusions contained in a specimen should vary by chance, whereas the fatigue limit is determined with several specimens as an averaged behavior. The data is plotted tentatively at 20 μm position, for steels revealing no inclusion at crack initiation site.

The relative fatigue strength is found to be 1.707 as mean for steels without inclusions, and with 0.038 as its standard deviation. For horizontal part of the data in the figure, solid and broken lines are traced using these data without inclusion, representing mean and 95% confidence intervals, respectively. It can be judged that the decrease of strength begins at the size of 45 μm. The inclined solid and broken lines are obtained by multi-variables analysis of data beyond 45 μm, by pooling them into three groups according to Vickers hardness of materials, as below 260, above 320, and in between. Hardness values of 230, 290 and 350 are labeled to each lines to represent the three groups.

Dash-dotted lines in the figure are the predictions by linear fracture mechanics theory assuming a hardness dependence of fatigue threshold[31]. The agreement of prediction to observation is not satisfactory, because of the incertitude of the hardness dependence of threshold data used in the analysis. Similar analyses have been attempted since then by different authors giving substantially the same trends.

It is also to be noted that the steel SNC631 shows obviously a higher fatigue strength in Fig. 33. This steel has nominal composition of 0.31C-2.7Ni-0.8Cr and presents a better quench hardenability as compared to the other steels at the same carbon content level.

Non-metallic inclusions in steels are generally evaluated by a microscopic test method in JIS. The method is in principle the area proportion counting on a metallurgical section of samples. Inclusions are classified in three categories: type A for those deformed by plastic work such as sulfide or silicate, type B for those appearing in discontinuous arrays like alumina, and type C for those found isolated as in case of granular oxides.

For the materials investigated in the present paper, the JIS value for each type was always less than 0.05% for any heat/lot, and less than 0.1% for total of three types. No correlation was found between these values and relative fatigue strength described above. It is clear that the size of large inclusions should be evaluated for better qualification of steels from fatigue point of view. One of the attempts for this is found in a new standard of non-metallic inclusions test method for spring steels[32].

6. Concluding Remarks

From NRIM FDS publications the data have been extracted and collectively analyzed in view of providing standard reference values on basic high-cycle fatigue properties of Japanese steels for machine structural use. Although the most of original data were obtained in 1975–1980, the statistical facts and findings are believed to be valid and applicable to a variety of materials at present.

It is however noted that the data refers only to the hot rolled bars of 19–22 mm in diameter, heat treated at this size, and fatigue tested as standard smooth specimens at room temperature in air. It is recommended to refer the fatigue properties in relative values to monotonic ones, as the effect of heat treatment may not be unique for different materials shape and size. Tables A1 to A4 in Appendix can be served for this purpose.

There was a rapid evolution in steel making processes in early 1980's in this country. Traditional ingot casting has been replaced by the continuous casting in most of companies. Secondary refining has become familiar today for high quality special steels. Therefore the information may not be the same as reported here, regarding the distribution in size and types of non-metallic inclusions.

The present paper is an extraction of the former publication in Japanese[24]. Comprehensive results of analysis are to be found there and direct reference of the original FDS will give further possibility of new findings. The FDS data is available through an on-line service of the factual materials databases by Japan Information Center of Science and Technology.

Acknowledgments

The author is greatly indebted to many colleagues of the National Research Institute for Metals who shared this enormous task of Fatigue Data Sheet Project. He appreciates the effort of his co-worker Akira Ishii who made all the related statistical analysis.

APPENDIX

Symbols

- A : Slope of S-N curve on log-log co-ordinates
- CD : Coefficient of variation in fatigue strength, %
- D : Knee point on S-N curve, $\log N_w$
- D_I : Ideal critical diameter, mm
- E_U : U-notch Charpy impact value, J/cm^2
- E_V : V-notch Charpy impact value, J/cm^2
- N_f : Number of cycles to failure
- N_w : Knee point on S-N curve, number of cycles
- n : Work hardening exponent
- T : Tempering temperature, °C
- δ : Elongation, %
- δ_U : Uniform elongation, %
- σ_B : Tensile strength, N/mm^2
- σ_s : Upper yield strength, N/mm^2
- σ_T : True fracture strength, N/mm^2
- σ_u : Fatigue limit under repeated tension, N/mm^2
- σ_w : Fatigue limit under reversed tension-compression, N/mm^2
- σ_{wb} : Fatigue limit under rotating bending, N/mm^2
- σ_{yc} : Cyclic yield strength, N/mm^2
- $\sigma_{0.0}$: 0.2% proof stress, N/mm^2
- τ_w : fatigue limit under reversed torsion, N/mm^2
- ϕ : Reduction in area, %

Table A1 (1). Mechanical properties of JIS steels for machine structural use, expressed as mean (upper) and standard deviation (lower)

Steel (No. of heat)	Temper temp (°C)	Tensile properties: Up yield strength (N/mm^2)	Proof stress (N/mm^2)	Tensile strength (N/mm^2)	True fract strength (N/mm^2)	Uniform elong'tn (%)	Elon-gation (%)	Reduction in area (%)	Work harde'ng exponent	Impact value: V-notch Charpy (J/cm^2)	U-notch Charpy (J/cm^2)	Vickers hard-ness
S25C (11)	Normal-ized	363 36	329 21	489 25	980 33	26.6 3.4	37.8 2.3	63.5 2.1	0.254 0.010	134 40	— —	142 7
S35C (12)	550	575 52	568 52	750 43	1469 46	10.7 1.2	22.3 2.3	67.1 3.8	0.192 0.025	188 28	— —	247 15
	600	525 38	519 38	697 28	1443 37	12.0 1.0	25.1 1.9	70.2 2.2	0.204 0.018	213 23	— —	227 11
	650	503 41	487 34	650 27	1407 45	14.0 1.0	28.1 1.3	71.9 2.0	0.216 0.017	233 22	— —	208 8
	550–650	535 53	525 54	699 53	1439 49	12.3 1.7	25.3 3.0	69.7 3.4	0.204 0.022	212 31	— —	227 20
S45C (11)	550	696 97	693 97	862 58	1550 52	9.4 1.1	20.9 1.8	62.1 3.5	0.162 0.040	122 32	— —	280 19
	600	630 79	625 76	789 40	1505 40	10.6 0.8	23.2 1.5	65.5 2.3	0.176 0.032	151 30	— —	255 15
	650	575 61	565 53	718 26	1455 41	12.5 0.7	26.6 1.1	68.5 1.6	0.191 0.022	174 25	— —	232 10
	550–650	634 94	628 93	790 73	1504 59	10.8 1.5	23.6 2.8	65.4 3.6	0.176 0.034	149 36	— —	255 25
S55C (11)	550	798 84	798 80	949 33	1589 44	8.0 0.8	18.9 1.5	57.0 2.9	0.130 0.036	86 10	— —	306 13
	600	709 63	708 61	850 19	1517 20	9.8 0.4	22.1 1.4	60.9 2.3	0.146 0.028	118 18	— —	275 9
	650	637 51	626 44	761 13	1450 21	11.8 0.6	25.3 1.1	64.1 1.6	0.165 0.020	146 17	— —	246 7
	550–650	712 93	711 94	853 81	1519 65	9.9 1.7	22.1 3.0	60.7 3.7	0.147 0.032	116 29	— —	276 26
SMn438 (7)	550	688 31	727 62	866 47	1594 46	8.3 0.8	19.3 1.5	63.3 3.4	0.136 0.018	142 25	172 25	283 14
	600	656 51	655 51	798 33	1541 39	9.9 1.1	22.0 1.6	66.3 1.9	0.156 0.017	168 23	197 18	259 12
	650	620 27	601 33	737 27	1515 34	11.7 0.6	24.8 1.2	69.2 1.7	0.172 0.014	195 20	226 19	239 9
	550–650	643 44	662 72	801 64	1548 50	10.0 1.6	22.2 2.7	66.5 3.3	0.155 0.022	168 31	199 30	260 22

Table A1 (2)

Steel (No. of heat)	Temper temp (°C)	Tensile properties								Impact value		Vickers hard-ness
		Up yield strength (N/mm^2)	Proof stress (N/mm^2)	Tensile strength (N/mm^2)	True fract strength (N/mm^2)	Uniform elong'tn (%)	Elon-gation (%)	Reduction in area (%)	Work harde'ng exponent	V-notch Charpy (J/cm^2)	U-notch Charpy (J/cm^2)	
SMn443 (12)	550	851 59	829 64	951 48	1640 38	8.2 0.7	18.8 1.3	60.2 2.7	0.114 0.014	108 17	131 25	305 10
	600	743 56	738 56	861 42	1575 28	9.6 0.6	21.2 1.4	63.2 2.4	0.139 0.012	134 20	163 22	277 10
	650	679 48	664 47	785 36	1543 38	11.6 0.5	24.5 1.1	66.8 1.9	0.161 0.014	166 18	195 18	250 10
	550–650	749 87	742 87	865 80	1585 53	9.8 1.6	21.6 2.6	63.4 3.5	0.138 0.023	136 30	163 34	277 25
SCr440 (8)	550	919 19	957 39	1054 35	1756 35	6.9 0.6	16.9 0.9	60.6 2.7	0.088 0.006	98 15	117 20	335 11
	600	854 24	840 31	956 29	1662 37	8.4 0.8	19.3 0.9	63.1 2.2	0.113 0.005	128 18	146 18	304 9
	650	753 18	753 19	874 16	1640 33	10.1 0.7	21.3 0.5	66.7 1.5	0.133 0.006	157 16	181 16	277 4
	550–650	790 64	850 90	961 79	1686 61	8.5 1.5	19.2 2.0	63.4 3.3	0.111 0.019	127 29	148 32	305 25
SCM435 (14)	550	1022 34	1017 37	1096 41	1818 50	7.1 0.6	16.6 1.0	61.9 2.5	0.078 0.006	111 27	132 30	352 10
	600	897 39	886 40	982 35	1741 50	8.2 0.8	18.7 1.2	65.5 2.8	0.100 0.007	145 25	174 29	318 9
	650	782 34	777 36	885 31	1710 48	10.1 1.1	21.4 1.3	69.1 2.7	0.127 0.007	189 27	214 31	285 9
	550–650	852 99	893 106	987 94	1756 67	8.5 1.5	18.9 2.3	65.5 4.0	0.101 0.021	148 41	173 45	318 29
SCM440 (15)	550	1055 22	1080 31	1164 34	1863 53	6.8 0.7	16.1 1.0	59.2 2.6	0.074 0.004	83 17	109 21	371 8
	600	936 27	950 30	1047 33	1775 44	7.8 1.0	17.9 1.2	62.3 2.3	0.096 0.005	115 19	145 25	335 7
	650	826 24	823 23	926 24	1691 63	9.8 1.4	20.9 1.1	65.8 1.7	0.125 0.006	156 24	188 19	298 7
	550–650	898 92	950 109	1046 102	1776 89	8.1 1.6	18.3 2.3	62.5 3.5	0.099 0.022	118 36	147 39	335 31

Table A1 (3)

Steel (No. of heat)	Temper temp (°C)	Tensile properties: Up yield strength (N/mm²)	Proof stress (N/mm²)	Tensile strength (N/mm²)	True fract strength (N/mm²)	Uniform elong'tn (%)	Elon-gation (%)	Reduction in area (%)	Work harde'ng exponent	Impact value: V-notch Charpy (J/cm²)	U-notch Charpy (J/cm²)	Vickers hard-ness
SNC631 (10)	550	912 32	925 36	1001 37	1751 42	7.1 0.5	18.9 1.1	64.7 2.3	0.088 0.009	123 25	148 36	316 11
	600	813 21	832 42	924 40	1704 32	8.3 0.6	21.0 1.3	67.2 1.9	0.114 0.011	152 20	176 32	292 11
	650	746 24	736 24	849 23	1678 30	10.0 0.5	23.4 0,8	70.2 1.5	0.146 0.009	183 19	213 29	267 7
	550–650	807 73	830 85	924 71	1710 46	8.5 1.3	21.1 2.1	67.4 2.9	0.117 0.026	153 33	179 42	292 22
SNCM439 (14)	580	1021 26	1033 35	1114 35	1830 44	7.1 0.4	17.2 1.0	60.5 1.5	0.090 0.009	98 11	116 13	351 10
	630	926 37	916 38	1003 34	1750 40	8.4 0.5	19.6 1.3	63.4 1.6	0.116 0.007	125 14	152 18	317 10
	680	820 27	779 17	874 20	1669 32	10.6 0.5	22.9 1.5	66.8 1.7	0.145 0.007	152 15	186 17	278 5
	580–630	905 83	908 109	996 103	1749 76	8.7 1.5	19.9 2.7	63.6 3.1	0.117 0.024	125 26	151 33	315 31
SNCM447 (6)	580	1032 31	1037 25	1131 33	1844 24	7.1 0.2	17.5 1.4	58.6 3.5	0.090 0.007	88 15	106 17	358 7
	630	920 16	912 18	1013 27	1767 19	8.6 0.2	20.3 1.6	62.6 2.3	0.117 0.005	114 20	140 22	321 5
	680	830 22	793 11	889 19	1656 32	10.5 0.2	23.4 1.6	64.6 3.0	0.141 0.008	142 20	173 22	286 4
	580–680	906 79	914 102	1011 103	1754 82	8.7 1.4	20.4 2.9	61.9 3.8	0.115 0.022	116 29	140 34	322 30
SUS403 (11)	700	— —	583 21	727 19	1449 60	8.4 0.7	24.0 1.1	70.8 2.0	0.112 0.015	— —	229 37	238 6
	750	— —	508 21	676 15	1426 50	11.3 0.9	27.3 1.7	72.4 1.4	0.126 0.010	— —	271 25	221 6
	700–750	— —	545 43	701 31	1438 56	9.9 1.7	25.7 2.2	71.7 1.9	0.119 0.014	— —	250 38	230 11
SUS430 (9)	Anneal-ed	306 26	301 25	494 20	1208 94	21.5 3.1	39.7 2.4	75.7 3.0	0.206 0.021	— —	135 108	170 10
SUS304 (11)	Solut'n treated	— —	257 17	614 32	1937 134	62.0 3.1	72.1 3.3	80.8 1.6	0.238 0.021	— —	— —	154 11

Table A2 (1). Fatigue strength and its ratios of JIS steels for machine structural use, expressed as mean (upper) and standard devision (lower)

Steel (No. of heat)	Temper temp (°C)	HV	σ_B (N/mm^2)	σ_{wb} (N/mm^2)	$\frac{\sigma_{wb}}{HV}$	$\frac{\sigma_{wb}}{\sigma_B}$	$\frac{\tau_w}{HV}$	$\frac{\tau_w}{\sigma_B}$	$\frac{\tau_w}{\sigma_{wb}}$	$\frac{\sigma_w}{HV}$	$\frac{\sigma_w}{\sigma_B}$	$\frac{\sigma_w}{\sigma_{wb}}$	$\frac{\sigma_w}{\sigma_u}$
S25C (11)	Normal-ized	142.1 6.9	489.2 23.8	242.5 14.1	1.707 0.066	0.496 0.020	1.031 0.040	0.301 0.008	0.618 0.010	1.518 0.036	0.443 0.016	0.910 0.018	1.178 0.045
S35C (12)	550	245.3 11.7	750.3 38.8	409.8 20.7	1.673 0.088	0.547 0.030	1.080 0.079	0.360 0.028	0.664 0.015				
	600	227.2 10.2	696.6 24.9	384.0 19.0	1.692 0.073	0.551 0.021	1.092 0.059	0.359 0.019	0.657 0.020	1.482 0.079	0.487 0.021	0.891 0.020	1.288 0.039
	650	207.5 7.9	649.6 24.8	350.9 20.6	1.692 0.086	0.540 0.024	1.092 0.040	0.354 0.015	0.668 0.036				
	550–650	226.6 18.4	698.8 51.0	381.6 31.3	1.685 0.081	0.546 0.025	1.088 0.056	0.358 0.020	0.663 0.023				
S45C (11)	550	280.0 18.2	861.9 57.4	472.4 30.3	1.688 0.058	0.548 0.017	1.126 0.077	0.369 0.024	0.679 0.046				
	600	254.5 14.2	789.7 39.0	434.5 21.9	1.708 0.030	0.550 0.010	1.137 0.073	0.365 0.022	0.671 0.041	1.616 0.077	0.519 0.029	0.954 0.042	1.303 0.028
	650	231.5 9.6	717.8 24.1	394.8 16.5	1.705 0.032	0.550 0.014	1.123 0.072	0.364 0.021	0.663 0.036				
	550–650	255.3 24.5	789.8 72.5	433.9 39.4	1.701 0.042	0.550 0.013	1.129 0.068	0.366 0.020	0.671 0.038				
S55C (11)	550	306.0 13.7	949.0 33.5	514.1 19.0	1.681 0.052	0.542 0.013	1.140 0.032	0.368 0.010	0.686 0.039				
	600	274.6 8.9	849.9 19.5	461.6 13.8	1.681 0.039	0.543 0.013	1.132 0.056	0.366 0.014	0.684 0.036	1.653 0.111	0.534 0.034	0.998 0.048	1.264 0.055
	650	246.5 6.6	760.9 12.6	413.3 10.1	1.678 0.047	0.543 0.015	1.097 0.042	0.355 0.010	0.664 0.041				
	550–650	275.7 26.6	853.3 81.3	463.0 44.2	1.680 0.045	0.543 0.013	1.123 0.045	0.363 0.012	0.678 0.036				
SMn438 (7)	550	282.7 13.2	871.4 39.3	457.6 32.6	1.618 0.080	0.525 0.024	1.159 0.050	0.378 0.015	0.707 0.023				
	600	259.3 11.3	803.7 28.0	425.9 20.7	1.643 0.065	0.530 0.019	1.127 0.023	0.366 0.008	0.697 0.012	1.574 0.105	0.512 0.035	0.973 0.033	1.243 0.033
	650	237.0 7.0	734.6 21.0	386.4 24.7	1.630 0.083	0.526 0.027	1.125 0.048	0.366 0.016	0.681 0.017				
	550–650	259.7 21.7	803.2 64.1	423.3 39.0	1.631 0.073	0.527 0.022	1.137 0.040	0.370 0.013	0.695 0.020				

Table A2 (2)

Steel (No. of heat)	Temper temp (°C)	HV	σ_B (N/mm^2)	σ_{wb} (N/mm^2)	$\frac{\sigma_{wb}}{HV}$	$\frac{\sigma_{wb}}{\sigma_B}$	$\frac{\tau_w}{HV}$	$\frac{\tau_w}{\sigma_B}$	$\frac{\tau_w}{\sigma_{wb}}$	$\frac{\sigma_w}{HV}$	$\frac{\sigma_w}{\sigma_B}$	$\frac{\sigma_w}{\sigma_{wb}}$	$\frac{\sigma_w}{\sigma_u}$
SMn443 (12)	550	304.7 9.4	950.1 46.6	499.3 37.0	1.637 0.078	0.525 0.019	1.110 0.052	0.358 0.013	0.674 0.021				
	600	276.7 10.1	865.5 40.6	461.0 32.8	1.665 0.073	0.532 0.018	1.142 0.030	0.364 0.011	0.676 0.017	1.629 0.087	0.519 0.022	0.694 0.036	1.265 0.022
	650	249.8 9.8	784.1 35.2	419.7 26.4	1.679 0.044	0.535 0.014	1.109 0.015	0.353 0.002	0.660 0.011				
	550–650	277.0 24.6	866.6 79.5	460.0 45.5	1.660 0.067	0.531 0.017	1.121 0.036	0.358 0.010	0.670 0.017				
SCr440 (8)	550	334.5 10.5	1054.4 32.5	553.8 21.8	1.657 0.087	0.525 0.022	1.153 0.060	0.367 0.016	0.691 0.026				
	600	304.1 7.7	954.6 26.6	507.6 7.4	1.670 0.042	0.532 0.013	1.126 0.064	0.361 0.014	0.680 0.016	1.664 0.054	0.533 0.004	1.005 0.025	1.249 0.021
	650	276.4 2.9	874.0 14.2	470.4 12.9	1.702 0.042	0.538 0.015	1.163 0.046	0.367 0.011	0.686 0.026				
	550–650	305.0 25.3	961.0 79.2	510.6 37.8	1.676 0.061	0.532 0.017	1.147 0.052	0.365 0.012	0.686 0.021				
SCM435 (14)	550	351.9 8.8	1095.8 37.4	556.4 27.1	1.609 0.056	0.517 0.015	1.100 0.021	0.357 0.008	0.697 0.041				
	600	317.1 9.1	981.6 32.5	528.4 24.4	1.666 0.059	0.538 0.015	1.137 0.021	0.369 0.010	0.693 0.033	1.629 0.044	0.529 0.015	0.993 0.036	1.240 0.044
	650	285.1 8.4	884.6 29.6	479.4 17.9	1.682 0.042	0.542 0.011	1.164 0.023	0.377 0.012	0.693 0.037				
	550–650	318.0 28.9	987.4 93.2	524.7 42.7	1.652 0.060	0.532 0.018	1.134 0.034	0.368 0.013	0.695 0.034				
SCM440 (15)	550	370.7 7.3	1163.5 31.9	600.5 26.4	1.620 0.062	0.516 0.019	1.077 0.061	0.346 0.026	0.680 0.069				
	600	335.2 7.0	1047.3 32.7	553.4 21.4	1.651 0.046	0.528 0.013	1.105 0.046	0.354 0.022	0.677 0.051	1.674 0.110	0.536 0.032	1.023 0.029	1.269 0.967
	650	297.9 6.1	925.7 23.8	498.7 11.4	1.674 0.030	0.539 0.010	1.131 0.050	0.366 0.021	0.680 0.030				
	550–650	334.6 30.8	1045.5 102.4	550.9 46.7	1.648 0.052	0.528 0.017	1.104 0.054	0.355 0.023	0.679 0.049				

Table A2 (3)

Steel (No. of heat)	Temper temp (°C)	HV	σ_B (N/mm^2)	σ_{wb} (N/mm^2)	$\frac{\sigma_{wb}}{HV}$	$\frac{\sigma_{wb}}{\sigma_B}$	$\frac{\tau_w}{HV}$	$\frac{\tau_w}{\sigma_B}$	$\frac{\tau_w}{\sigma_{wb}}$	$\frac{\sigma_w}{HV}$	$\frac{\sigma_w}{\sigma_B}$	$\frac{\sigma_w}{\sigma_{wb}}$	$\frac{\sigma_w}{\sigma_u}$
SNC631 (10)	550	315.7 11.6	1002.5 36.3	556.5 19.6	1.764 0.052	0.555 0.016	1.122 0.025	0.355 0.006	0.629 0.016				
	600	291.8 10.5	927.1 37.2	518.0 14.7	1.777 0.061	0.559 0.020	1.147 0.002	0.362 0.003	0.650 0.017	1.792 0.033	0.566 0.008	1.015 0.018	1.267 0.057
	650	267.2 7.2	849.1 23.3	483.7 11.6	1.811 0.047	0.570 0.016	1.148 0.036	0.364 0.010	0.640 0.030				
	550–650	291.6 22.5	926.2 71.2	519.4 33.8	1.784 0.055	0.561 0.018	1.139 0.025	0.360 0.007	0.636 0.022				
SNCM439 (14)	580	350.6 9.7	1113.9 35.6	593.4 23.0	1.692 0.044	0.533 0.016	1.145 0.026	0.360 0.008	0.674 0.006				
	630	317.2 10.0	1002.4 35.4	547.6 22.4	1.727 0.062	0.547 0.022	1.169 0.024	0.369 0.011	0.680 0.018	1.792 0.056	0.566 0.015	1.043 0.041	1.318 0.023
	680	278.0 4.6	874.7 20.0	478.9 12.2	1.722 0.032	0.548 0.011	1.192 0.038	0.378 0.011	0.684 0.017				
	580–680	315.3 31.2	997.0 103.5	540.0 51.4	1.714 0.049	0.542 0.018	1.169 0.034	0.369 0.012	0.679 0.014				
(6)	580	357.7 6.0	1131.3 34.5	594.0 15.9	1.661 0.056	0.525 0.022	1.101 0.043	0.349 0.023	0.657 0.012				
	630	320.8 5.4	1012.8 28.3	540.5 9.8	1.685 0.042	0.534 0.018	1.147 0.023	0.363 0.014	0.667 0.002	1.734 0.007	0.549 0.013	1.008 0.014	1.276 0.011
	680	285.5 3.7	889.0 19.7	475.2 6.6	1.665 0.031	0.535 0.016	1.137 0.013	0.362 0.001	0.688 0.026				
	580–680	321.3 30.7	1011.1 105.2	536.6 51.1	1.670 0.043	0.531 0.018	1.128 0.031	0.358 0.014	0.671 0.019				
SUS403 (11)	700	237.9 6.1	726.8 19.5	425.1 16.1	1.787 0.068	0.585 0.018	1.153 0.026	0.383 0.010	0.646 0.025	1.738 0.024	0.577 0.012	0.974 0.045	1.305 0.021
	750	220.5 5.6	676.2 14.8	399.5 16.6	1.812 0.056	0.591 0.016	1.147 0.027	0.376 0.006	0.628 0.020				
	700–750	229.2 10.6	701.5 30.9	412.3 20.6	1.800 0.062	0.588 0.017	1.150 0.025	0.379 0.009	0.637 0.023				
SUS430 (9)	Annealed	169.9 8.6	493.9 20.0	301.6 13.5	1.777 0.071	0.611 0.016	1.283 0.079	0.449 0.005	0.724 0.031	1.759 0.068	0.616 0.009	0.993 0.018	1.352 0.042
SUS304 (11)	Solut'n treated	154.0 9.9	613.9 32.7	301.7 10.0	1.963 0.081	0.492 0.023	1.015 0.029	0.259 0.008	0.514 0.009	1.485 0.080	0.379 0.009	0.752 0.026	1.130 0.020

Table A3 (1). Parameters for *S-N* curves of JIS steels for machine structural use, expressed as mean (upper) and standard devitation (lower). See equation (4)

Steel (No. of heat)	Temper temp (°C)	Tensile strength (N/mm^2)	Rotating bending					Reversed torsion				
			Number of *S-N* curve	Slope A	Fatigue limit σ_{wb} (N/mm^2)	Knee point D	Coeff. variat'n (%)	Number of *S-N* curve	Slope A	Fatigue limit τ_w (N/mm^2)	Knee point D	Coeff. variat'n (%)
S25C (11)	Normal-ized	489.2 23.8	11	0.0540 0.0047	24.25 14.1	6.596 0.100	1.92 0.78	4	0.0702 0.0024	145.0 5.1	6.794 0.127	4.99 0.73
S35C (12)	550	750.3 38.8	12	0.0610 0.0163	409.8 20.7	6.049 0.075	3.91 2.23	4	0.0402 0.0214	265.0 9.6	6.242 0.076	5.79 4.97
	600	696.6 24.9	12	0.0589 0.0132	384.0 19.0	6.071 0.176	3.87 1.92	4	0.0410 0.0082	248.3 6.6	6.148 0.469	6.52 3.77
	650	649.6 24.8	12	0.0549 0.0093	350.9 20.6	6.222 0.221	3.62 1.66	4	0.0369 0.0179	226.8 7.1	6.394 0.369	5.62 3.27
	550–650	698.8 51.0	36	0.0583 0.0131	381.6 31.3	6.114 0.181	3.80 1.90	12	0.0394 0.0153	246.7 17.8	6.261 0.331	5.98 3.70
S45C (11)	550	861.9 57.4	11	0.0647 0.0137	472.4 30.3	5.879 0.184	3.23 1.91	4	0.0326 0.0111	313.0 4.5	6.627 0.391	4.10 2.34
	600	789.7 39.0	11	0.0561 0.0101	434.5 21.9	6.026 0.184	3.08 1.71	4	0.0350 0.0152	286.5 5.0	6.420 0.039	3.92 1.91
	650	717.8 24.1	11	0.0529 0.0064	394.8 16.5	6.145 0.180	2.67 1.61	4	0.0371 0.0079	260.3 6.7	6.338 0.182	3.51 1.01
	550–650	789.8 72.5	33	0.0579 0.0114	433.9 39.4	6.016 0.209	2.99 1.71	12	0.0349 0.0108	286.6 23.0	6.461 0.259	3.84 1.68
S55C (11)	550	949.0 33.5	11	0.0758 0.0150	514.1 19.0	5.841 0.155	2.79 1.38	4	0.0381 0.0142	348.8 9.4	6.421 0.521	3.36 0.57
	600	849.9 19.5	11	0.0685 0.0070	461.6 13.8	5.935 0.124	2.38 0.76	4	0.0349 0.0120	309.5 8.3	6.593 0.374	3.23 0.55
	650	760.9 12.6	11	0.0594 0.0112	413.3 10.1	6.052 0.079	2.26 1.31	4	0.0331 0.034	270.0 10.4	6.604 0.353	2.92 0.65
	550–650	853.3 81.3	33	0.0679 0.0131	463.0 44.2	5.943 0.148	2.48 1.17	12	0.0354 0.0101	309.4 34.6	6.539 0.392	3.17 0.57
SMn438 (7)	550	871.4 39.3	7	0.0828 0.0221	457.6 32.6	5.946 0.239	6.03 2.70	3	0.0386 0.0106	335.3 27.1	6.097 0.108	4.75 3.45
	600	803.7 28.0	7	0.0715 0.0153	425.9 20.7	6.067 0.231	5.61 3.55	3	0.0429 0.0124	298.7 16.5	6.318 0.157	6.86 3.33
	650	734.6 21.0	7	0.0660 0.0100	386.4 24.7	6.255 0.272	4.53 2.28	3	0.0400 0.0125	272.3 15.7	6.299 0.235	4.71 2.85
	550–650	803.2 64.1	21	0.0734 0.0172	423.3 39.0	6.090 0.269	5.39 2.82	9	0.0405 0.0104	302.1 32.6	6.238 0.184	5.44 2.99

Table A3 (2)

Steel (No. of heat)	Temper temp (°C)	Tensile strength (N/mm^2)	Rotating bending: Number of S-N curve	Slope A	Fatigue limit σ_{wb} (N/mm^2)	Knee point D	Coeff. variat'n (%)	Reversed torsion: Number of S-N curve	Slope A	Fatigue limit τ_w (N/mm^2)	Knee point D	Coeff. variat'n (%)
SMn443 (12)	550	950.1 46.6	12	0.0783 0.0107	499.3 37.0	5.948 0.167	3.88 2.27	4	0.0380 0.0125	336.8 20.1	6.512 0.281	5.81 1.93
	600	865.5 40.6	12	0.733 0.0101	461.0 32.8	5.997 0.168	3.52 2.46	4	0.0393 0.0101	312.5 15.0	6.191 0.053	5.52 1.09
	650	784.1 35.2	12	0.673 0.0083	419.7 26.4	6.090 0.174	3.05 1.53	4	0.0386 0.0049	273.8 13.5	6.539 0.200	4.76 1.64
	550–650	866.6 79.5	36	0.0730 0.0105	460.0 45.5	6.012 0.175	3.48 2.09	12	0.0386 0.0088	307.7 30.9	6.414 0.246	5.36 1.51
SCr440 (8)	550	1054.4 32.5	8	0.1047 0.0216	553.8 21.8	5.786 0.221	4.66 3.01	3	0.0423 0.0130	383.7 14.6	6.423 0.207	3.99 2.00
	600	954.6 26.6	8	0.0829 0.0215	507.6 7.4	5.993 0.192	3.27 1.64	3	0.0584 0.0101	342.7 11.7	6.305 0.250	4.38 0.26
	650	874.0 14.2	8	0.741 0.0093	470.4 12.9	6.025 0.065	2.91 1.68	3	0.0349 0.0027	320.3 14.6	6.535 0.167	3.10 1.24
	550–650	961.0 79.2	24	0.0872 0.0219	510.6 37.8	5.935 0.198	3.61 2.24	9	0.0452 0.0133	348.9 30.2	6.421 0.208	3.82 1.31
SCM435 (14)	550	1095.8 37.4	14	0.1055 0.0143	566.4 27.1	5.831 0.103	4.74 2.16	5	0.0471 0.0124	384.4 12.9	6.507 0.294	4.02 0.88
	600	981.6 32.5	14	0.0933 0.0133	528.4 24.4	5.873 0.103	3.58 1.76	5	0.0427 0.0072	355.8 11.0	6.428 0.155	5.17 1.95
	650	884.6 29.6	14	0.0876 0.0133	479.4 17.9	5.950 0.155	3.26 1.03	5	0.0382 0.0033	325.0 12.2	6.420 0.328	3.87 1.83
	550–650	987.4 93.2	42	0.0955 0.0153	524.7 42.7	5.885 0.130	3.86 1.79	15	0.0427 0.0087	355.1 27.5	6.452 0.253	4.36 1.62
SCM440 (15)	550	1163.5 31.9	15	0.1069 0.0122	600.5 26.4	5.747 0.126	4.72 2.72	5	0.0545 0.0153	403.2 20.2	6.381 0.146	4.63 1.18
	600	1047.3 32.7	15	0.1015 0.0207	553.4 21.4	5.802 0.159	3.89 1.88	5	0.0566 0.0080	374.2 14.0	6.270 0.254	4.30 0.71
	650	925.7 23.8	15	0.0806 0.0129	498.7 11.4	5.982 0.106	2.91 0.87	5	0.0533 0.0133	338.2 8.3	6.150 0.208	3.11 0.76
	550–650	1045.5 102.4	45	0.0963 0.0192	550.9 46.7	5.844 0.164	3.84 2.07	15	0.0548 0.0117	371.9 30.8	6.267 0.215	4.01 1.08

Table A3 (3)

Steel (No. of heat)	Temper temp (°C)	Tensile strength (N/mm^2)	Rotating bending: Number of S-N curve	Slope A	Fatigue limit σ_{wb} (N/mm^2)	Knee point D	Coeff. variat'n (%)	Reversed torsion: Number of S-N curve	Slope A	Fatigue limit τ_w (N/mm^2)	Knee point D	Coeff. variat'n (%)
SNC631 (10)	550	1002.5 36.3	10	0.0926 0.0217	556.5 19.6	5.874 0.123	3.69 1.23	3	0.0574 0.0073	349.0 17.1	6.374 0.114	3.94 0.86
	600	927.1 37.2	10	0.0767 0.0084	518.0 14.7	6.070 0.213	3.03 0.71	3	0.0474 0.0058	330.0 9.5	6.457 0.132	3.53 0.36
	650	849.1 23.3	10	0.754 0.0076	483.7 11.6	6.013 0.168	2.56 0.92	3	0.485 0.0056	304.7 11.5	6.440 0.068	3.00 0.52
	550–650	926.2 71.2	30	0.0816 0.0158	519.4 33.8	5.986 0.186	3.09 1.05	9	0.0511 0.0072	327.9 22.4	6.424 0.101	3.49 0.67
SNCM439 (14)	580	1113.9 35.6	14	0.0990 0.0158	593.4 23.0	5.812 0.124	3.40 1.54	4	0.0449 0.0061	396.8 8.8	6.422 0.134	4.03 1.22
	630	1002.4 35.4	14	0.0891 0.0133	547.6 22.4	5.860 0.177	3.15 1.24	4	0.0474 0.0136	365.5 8.7	6.297 0.281	3.60 0.86
	680	874.7 20.0	14	0.0717 0.0158	478.9 12.2	6.111 0.168	2.70 1.17	4	0.0309 0.0066	328.5 12.9	6.345 0.142	2.82 0.83
	580–680	997.0 103.5	42	0.0866 0.0186	540.0 51.4	5.928 0.203	3.08 1.33	12	0.0411 0.0114	363.6 30.6	6.355 0.186	3.48 1.03
SNCM447 (6)	580	1131.3 34.5	6	0.1040 0.0160	594.0 15.9	5.737 0.137	6.82 3.54	2	0.0574 0.0090	393.5 16.3	6.396 0.075	4.95 0.63
	630	1012.8 28.3	6	0.0933 0.147	540.5 9.8	5.857 0.099	4.24 2.48	2	0.0470 0.0128	367.0 4.2	6.345 0.206	2.29 1.14
	680	889.0 19.7	6	0.0742 0.0103	475.2 6.6	6.094 0.095	3.11 1.78	2	0.0355 0.0082	323.5 9.2	6.448 0.481	3.24 0.11
	580–680	1011.1 105.2	18	0.0905 0.0182	536.6 51.1	5.896 0.185	4.72 3.00	6	0.466 0.0127	361.3 32.8	6.396 0.241	3.49 1.34
SUS403 (11)	700	726.8 19.5	11	0.0639 0.0078	425.1 16.1	6.239 0.213	2.19 0.61	4	0.0376 0.0042	274.3 10.8	6.743 0.301	2.45 0.53
	750	676.2 14.8	11	0.0552 0.0067	399.5 16.6	6.287 0.170	2.50 0.85	4	0.0380 0.0049	252.0 3.4	6.911 0.147	3.19 0.56
	700–750	701.5 30.9	22	0.0595 0.0083	412.3 20.6	6.263 0.190	2.35 0.74	8	0.0378 0.0042	263.1 14.0	6.827 0.237	2.82 0.64
SUS430 (9)	Anneal-ed	493.9 20.0	9	0.0585 0.134	301.6 13.5	6.723 0.119	2.86 0.83	3	0.0460 0.0036	218.3 1.5	6.913 0.087	4.20 0.69
SUS304 (11)	Solut'n treated	613.9 32.7	11	0.0539 0.0074	301.7 10.0	5.417 0.162	2.14 0.81	4	0.0367 0.0051	156.8 5.9	5.862 0.401	2.72 1.57

Table A3 (4)

Steel (No. of heat)	Temper temp (°C)	Tensile strength (N/mm^2)	Reversed tension-compression: Number of *S-N* curve	Slope A	Fatigue limit σ_w (N/mm^2)	Knee point D	Coeff. variat'n (%)	Repeated tension: Number of *S-N* curve	Slope A	Fatigue limit σ_u (N/mm^2)	Knee point D	Coeff. variat'n (%)
S25C (11)	Normal-ized	489.2 23.8	4	0.0732 0.0233	213.5 5.8	5.925 0.301	3.55 1.41	4	0.0449 0.0167	181.3 3.3	6.688 0.218	3.05 1.88
S35C (12)	600	696.6 24.9	4	0.0428 0.0095	337.0 14.9	5.718 0.369	4.75 2.47	4	0.0627 0.0063	261.8 12.5	6.126 0.191	4.20 2.08
S45C (11)	600	789.7 39.0	4	0.0415 0.0198	408.5 37.6	5.613 0.644	2.46 0.34	4	0.0487 0.0214	313.5 27.1	6.101 0.434	2.46 0.39
S55C (11)	600	849.9 19.5	4	0.0312 0.0092	452.3 30.6	5.788 0.274	2.89 1.28	4	0.0317 0.0164	358.0 25.0	5.894 0.679	2.35 0.46
SMn438 (7)	600	803.7 28.0	3	0.0349 0.0271	417.7 42.7	6.250 0.322	6.08 5.72	3	0.0511 0.0234	335.7 26.0	5.792 0.151	4.83 4.29
SMn443 (12)	600	865.5 40.6	4	0.0473 0.0178	446.0 39.5	5.668 0.255	4.73 3.35	4	0.0341 0.0119	352.5 30.7	6.208 0.070	4.67 2.79
SCr440 (8)	600	954.6 26.6	3	0.0378 0.0172	506.7 18.8	5.777 0.146	4.51 3.93	3	0.0408 0.0104	405.7 9.5	5.857 0.099	3.75 3.32
SCM435 (14)	600	981.6 32.5	5	0.0430 0.0093	509.8 14.0	6.130 0.390	5.01 2.15	5	0.0441 0.0087	411.4 15.9	5.973 0.434	4.26 2.83
SCM440 (15)	600	1047.3 32.7	5	0.0368 0.0143	567.6 44.5	5.968 0.475	3.70 1.89	5	0.0534 0.0206	447.4 27.5	5.877 0.297	3.84 2.22
SNC631 (10)	600	927.1 37.2	3	0.0321 0.0086	515.3 11.0	6.260 0.052	2.35 0.09	3	0.0406 0.0122	407.3 24.0	5.798 0.145	1.60 0.36
SNCM439 (14)	630	1002.4 35.4	4	0.0344 0.0100	560.3 13.7	5.938 0.078	2.10 0.56	4	0.0343 0.0111	425.3 16.3	6.088 0.082	1.82 0.65
SNCM447 (6)	630	1012.8 28.3	2	0.0322 0.0062	555.0 2.8	6.130 0.099	2.16 0.43	2	0.0290 0.0177	435.0 1.4	6.035 0.375	1.76 0.63
SUS403 (11)	700	726.8 19.5	4	0.0297 0.0057	413.3 15.3	6.123 0.298	2.17 0.97	4	0.0499 0.0140	316.8 11.8	5.947 0.276	2.96 0.30
SUS430 (9)	Anneal-ed	493.9 20.0	3	0.0180 0.0025	299.7 8.4	6.513 0.422	2.03 0.41	3	0.0481 0.0372	222.0 13.0	6.445 0.114	2.77 0.63
SUS304 (11)	Solut'n treated	613.9 32.7	4	0.0701 0.0281	229.3 11.4	5.178 0.216	3.44 0.60	4	0.1499 0.0747	203.0 11.5	5.653 0.113	4.22 1.55

Table A4 (1). Parameters for normalized *S-N* curves of JIS steels for machine structural use. See equation (4)

Steel (No. of heat)	Temper temp (°C)	Loading condi-tion	Number of data	Relative to tensile strength				Relative to Vickers hardness			
				Slope A	Fatigue limit σ/σ_B	Knee point D	Coeff. variat'n (%)	Slope A	Fatigue limit σ/HV	Knee point D	Coeff. variat'n (%)
S25C	Normal-ized	Rot. bend	207	0.0596	0.5061	6.3981	6.457	0.0555	1.7253	6.5059	4.987
		Torsion	70	0.0642	0.3034	6.9050	5.511	0.0669	1.0241	6.9250	6.405
		Tens. comp.	66	0.0767	0.4402	5.8533	5.842	0.0688	1.5166	5.9156	4.565
		Zero Tens.	62	0.0413	0.3785	6.5854	4.234	0.0466	1.2641	6.7103	5.013
S35C	550–650	Rot. bend	745	0.0630	0.5516	5.9902	5.971	0.0638	1.6988	5.9965	6.338
	550–650	Torsion	213	0.0453	0.3642	5.9362	7.786	0.0479	1.0995	5.9888	8.413
	600	Tens. comp.	59	0.0469	0.4938	5.5955	6.418	0.0523	1.5025	5.5729	7.395
	600	Zero Tens.	61	0.0583	0.3865	6.0453	5.178	0.0678	1.1719	6.0036	6.746
S45C	550–650	Rot. bend	667	0.0509	0.5598	6.0827	4.495	0.0505	1.7074	6.0745	4.655
	550–650	Torsion	211	0.0389	0.3678	6.2866	6.351	0.0406	1.1377	6.2392	7.183
	600	Tens. comp.	58	0.0507	0.5187	5.3256	7.232	0.0445	1.6280	5.3247	6.176
	600	Zero Tens.	62	0.0802	0.4014	5.5728	5.401	0.0536	1.2466	5.8393	5.209
S55C	550–650	Rot. bend	652	0.0632	0.5396	6.0326	3.600	0.0644	1.6792	5.9751	3.454
	550–650	Torsion	214	0.0379	0.3634	6.3783	4.717	0.0368	1.1169	6.4943	5.459
	600	Tens. comp.	60	0.0371	0.5303	5.8277	7.123	0.0376	1.6151	6.0054	7.175
	600	Zero Tens.	60	0.0502	0.4268	5.5576	4.401	0.0296	1.2967	6.1250	3.822
SMn438	550–650	Rot. bend	405	0.0689	0.5247	6.1613	6.779	0.0702	1.6446	6.0696	7.152
	550–650	Torsion	166	0.0421	0.3709	6.1752	6.646	0.0428	1.1333	6.2285	7.010
	600	Tens. comp.	50	0.0508	0.5214	5.7385	10.643	0.0501	1.5999	5.7437	10.366
	600	Zero Tens.	41	0.0702	0.4134	5.6219	6.490	0.0673	1.2608	5.6986	5.872
SMn443	550–650	Rot. bend	685	0.0692	0.5270	6.1067	5.021	0.0701	1.6533	6.0868	5.877
	550–650	Torsion	210	0.0362	0.3610	6.3754	5.824	0.0369	1.1289	6.3628	6.260
	600	Tens. comp.	68	0.0462	0.5233	5.6182	6.694	0.0527	1.6413	5.5705	7.510
	600	Zero Tens.	57	0.0440	0.4171	5.8966	5.867	0.0506	1.3080	5.8099	6.935
SCr440	550–650	Rot. bend	453	0.0800	0.5312	5.9819	4.808	0.0815	1.6649	5.996	5.144
	550–650	Torsion	155	0.0396	0.3652	6.5428	5.090	0.0427	1.1443	6.5205	6.122
	600	Tens. comp.	49	0.0403	0.5355	5.6353	5.101	0.0444	1.6431	5.7166	5.829
	600	Zero Tens.	49	0.0429	0.4397	5.5066	5.721	0.0435	1.3239	5.9066	5.231
SCM435	550–650	Rot. bend	829	0.0950	0.5310	5.8906	5.378	0.0918	1.6442	5.9318	5.747
	550–650	Torsion	277	0.0400	0.3680	6.5353	5.346	0.0388	1.1325	6.5715	5.172
	600	Tens. comp.	82	0.0405	0.5385	5.9839	5.579	0.0391	1.6334	6.1589	5.700
	600	Zero Tens.	78	0.0493	0.4311	5.8153	5.272	0.0511	1.3071	5.9231	5.661
SCM440	550–650	Rot. bend	897	0.0925	0.5273	5.8660	6.193	0.0873	1.6362	5.9442	6.164
	550–650	Torsion	280	0.0642	0.3608	6.0746	8.291	0.0584	1.1200	6.1150	6.238
	600	Tens. comp.	81	0.0419	0.5364	5.9277	6.344	0.0452	1.6684	5.9200	6.699
	600	Zero Tens.	81	0.0481	0.4264	5.8667	6.206	0.0464	1.3091	6.0649	5.923
SNC631	580–680	Rot. bend	581	0.0801	0.5613	5.9933	4.012	0.0821	1.7892	5.9522	4.112
	580–680	Torsion	172	0.0475	0.3619	6.4441	3.864	0.0475	1.1453	6.4437	3.900
	630	Tens. comp.	45	0.0320	0.5657	6.3249	2.992	0.0315	1.7812	6.3860	2.912
	630	Zero Tens.	47	0.0412	0.4465	5.8151	4.005	0.0388	1.4094	5.8806	3.651

Table A4 (2)

Steel (No. of heat)	Temper temp (°C)	Loading condi-tion	Number of data	Relative to tensile strength: Slope A	Fatigue limit σ/σ_B	Knee point D	Coeff. variat'n (%)	Relative to Vickers hardness: Slope A	Fatigue limit σ/HV	Knee point D	Coeff. variat'n (%)
SNCM439	580–680	Rot. bend	800	0.0797	0.5356	6.0506	5.018	0.0783	1.6840	6.0848	4.734
	580–680	Torsion	213	0.0418	0.3704	6.3279	4.466	0.0399	1.1653	6.3942	4.043
	630	Tens. comp.	68	0.0298	0.5625	6.1766	2.758	0.0403	1.7919	5.8127	2.980
	630	Zero Tens.	63	0.0380	0.4383	5.7608	2.390	0.0404	1.3771	5.7953	3.016
SNCM447	580–680	Rot. bend	355	0.0831	0.5259	6.0109	6.712	0.0800	1.6495	6.0482	5.903
	580–680	Torsion	113	0.0457	0.3561	6.4738	6.175	0.0464	1.1216	6.4254	4.831
	630	Tens. comp.	33	0.0486	0.5446	5.9261	5.085	0.0344	1.7363	6.0805	2.817
	630	Zero Tens.	31	0.0261	0.4293	6.0670	2.595	0.0259	1.3555	6.0772	2.305
SUS403	700–750	Rot. bend	315	0.0600	0.5816	6.3234	3.042	0.0608	1.7748	6.3390	3.399
	700–750	Torsion	132	0.0380	0.3836	6.6910	3.286	0.0378	1.1511	6.8165	3.479
	700	Tens. comp.	56	0.0307	0.5724	6.2157	2.330	0.0309	1.7289	6.1599	2.464
	700	Zero Tens.	56	0.0480	0.4395	5.9885	3.238	0.0501	1.3260	5.9591	3.897
SUS430	Anneal-ed	Rot. bend	138	0.0587	0.6114	6.7337	4.553	0.0658	1.7666	6.7196	6.956
		Torsion	50	0.0455	0.4447	7.0002	4.010	0.0544	1.2547	6.9269	7.895
		Tens. comp.	39	0.0203	0.6169	6.4798	4.001	0.0026	1.7470	6.4824	5.342
		Zero Tens.	39	0.0542	0.4583	6.2960	4.223	0.0566	1.3067	6.3106	5.435
SUS304	Solut'n treated	Rot. bend	141	0.0574	0.4921	5.4363	5.636	0.0612	1.9661	5.4133	6.268
		Torsion	35	0.0360	0.2629	5.7347	5.915	0.0389	1.0182	5.8252	4.486
		Tens. comp.	52	0.0587	0.3754	5.3394	3.293	0.0562	1.4545	5.5110	6.133
		Zero Tens.	55	0.1209	0.3293	5.7501	4.115	0.1236	1.2846	5.7529	7.083

References

1) Program of the Fatigue Data Sheet Project for Engineering Materials Manufactured in Japan, NRIM Fatigue Data Sheet, No. 0 (1978), pp. 8.
2) Data Sheet on Fatigue Properties of S25C (0.25C) Steel for Machine Structural Use, NRIM Fatigue Data Sheet, No. 1 (1978), pp. 8.
3) Data Sheet on Fatigue Properties of S35C (0.35C) Steel for Machine Structural Use, NRIM Fatigue Data Sheet, No. 2 (1978), pp. 14.
4) Data Sheet on Fatigue Properties of S45C (0.45C) Steel for Machine Structural Use, NRIM Fatigue Data Sheet, No. 3 (1978), pp. 14.
5) Data Sheet on Fatigue Properties of S55C (0.55C) Steel for Machine Structural Use, NRIM Fatigue Data Sheet, No. 4 (1978), pp. 14.
6) Data Sheet on Fatigue Properties of SCr440 (0.40C-1Cr) Steel for Machine Structural Use, NRIM Fatigue Data Sheet, No. 8 (1979), pp. 14.
7) Data Sheet on Fatigue Properties of SCM435 (0.35C-1Cr-0.2Mo) Steel for Machine Structural Use, NRIM Fatigue Data Sheet, No. 9 (1979), pp. 16.
8) Data Sheet on Fatigue Properties of SCM440 (0.40C-1Cr-0.2Mo) Steel for Machine Structural Use, NRIM Fatigue Data Sheet, No. 10 (1979), pp. 16.
9) Data Sheet on Fatigue Properties of SMn 438 (0.38C-1.5Mn) Steel for Machine Structural Use, NRIM Fatigue Data Sheet, No. 16 (1980), pp. 14.
10) Data Sheet on Fatigue Properties of SMn443 (0.43C-1.5Mn) Steel for Machine Structural Use, NRIM Fatigue Data Sheet, No. 17 (1980), pp. 14.
11) Data Sheet on Fatigue Properties of SNC631 (0.31C-2.7Ni-0.8Cr) Steel for Machine Structural Use, NRIM Fatigue Data Sheet, No. 24 (1981), pp. 14.
12) Data Sheet on Fatigue Properties of SNCM439 (0.39C1.8Ni-0.8Cr-0.2Mo) Steel for Machine Structural Use, NRIM Fatigue Data Sheet, No. 25 (1981), pp. 16.
13) Data Sheet on Fatigue Properties of SNCM447 (0.47C-1.8Ni-0.8Cr-0.2Mo) Steel for Machine Structural Use, NRIM Fatigue Data Sheet, No. 26 (19819, pp. 12.
14) Data Sheet on Fatigue Properties of SUS430 (17Cr) Stainless Steel Bars for Machine Structural Use, NRIM Fatigue Data Sheet, No. 29 (1982), pp. 8.
15) Data Sheet on Fatigue Properties of SUS403 (12Cr) Stainless Steel Bars for Machine Structural Use, NRIM Fatigue Data Sheet, No. 30 (1982), pp. 12.

16) Data Sheet on Fatigue Properties of SUS303 (18Cr-8Ni) Stainless Steel Bars for Machine Structural Use, NRIM Fatigue Data Sheet, No. 33 (1983), pp. 10.
17) Data Sheet on Low-Cycle Fatigue Properties of S25C (0.25C) Steel for Machine Structural Use, NRIM Fatigue Data Sheet, No. 38 (1984), pp. 8.
18) Data Sheet on Low-Cycle Fatigue Properties of S35C (0.35C) Steel for Machine Structural Use, NRIM Fatigue Data Sheet, No. 39 (1984), pp. 18.
19) Data Sheet on Low-Cycle Fatigue Properties of S45C (0.45C) Steel for Machine Structural Use, NRIM Fatigue Data Sheet, No. 44 (1985), pp. 18.
20) Data Sheet on Low-Cycle Fatigue Properties of SCr440 (0.40C-1Cr) Steel for Machine Structural Use, NRIM Fatigue Data Sheet, No. 45 (1985), pp. 14.
21) Data Sheet on Low-Cycle Fatigue Properties of SCM435 (0.35C-1Cr-0.2Mo) Steel for Machine Structural Use, NRIM Fatigue Data Sheet, No. 52 (1986), pp. 16.
22) Data Sheet on Low-Cycle Fatigue Properties of SNCM439 (0.39C-1.8Ni1Cr-0.2Mo) Steel for Machine Structural Use, NRIM Fatigue Data Sheet, No. 56 (1987), pp. 16.
23) Nishijima, S., Mechanical Properties and Fatigue Strength of JIS Carbon, Chromium and Chromium-Molybdenum Steels for Machine Structural Use, NRIM Fatigue Data Sheet Technical Document, in Japanese, No. 1 (1981), pp. 93.
24) Nishijima, S., Ishii, A., Kanazawa, K., Matsuoka, S., and Masuda, C., Fundamental Fatigue Properties of JIS Steels for Machine Structural Use, NRIM Fatigue Data Sheet Technical Documents, in Japanese, No. 5 (1989), pp. 161.
25) Nishijima, S., Statistical Analysis of Small Sample Fatigue Data, in "Statistical Research on Fatigue and Fracture", Tanaka, T., Nishijima, S., and Ichikawa, M., Eds, Current Japanese Materials Research, Soc. Mat. Sci., Japan, Vol. 2 (1987), pp. 1–19, Elsevier Applied Sci.
26) Nishijima, S. and Ishii, A., Parametric Representation and Analysis of S-N Data with Bi-Linear Curve Fitting, Trans. NRIM, 29 (1987), pp. 21–29.
27) Standard Method of Statistical Fatigue Testing, JSME S002–81 (1981), pp. 159, Japan Soc. Mech. Engineers.
28) Takeuchi, E., Matsuoka, S., and Nishijima, S., Fatigue Properties of SUS304 Steel at Room Temperature in Laboratory Air, Trans. NRIM, 30 (1988), pp. 138–145.
29) Tanaka, K., Nishijima, S., Matsuoka, S., Abe, T., and Kouzu, F., Low- and High-Cycle Fatigue Properties of Various Steels Specified in JIS for Machine Structural Use, Fatigue Engng. Mat. Struct., 4 (1981), pp. 97–108.
30) ASTM A 255–1967, Standard Method of End-Quench Test for Hardenability of Steels, (1967).
31) Nishijima, S., Tanaka, K., and Sumiyoshi, H., Proc. 6th Int. Conf. Fracture, India, 3 (1984), 1719.
32) JSMA Standard, Microscopic Testing Method of Non-Metallic Inclusions for Spring Steels, Spring Manufacturers Assoc., Japan.

Basic Fatigue Properties of JIS Steels
for Machine Structural Use

by

Satoshi NISHIJIMA

NRIM Special Report
(Technical Report)
No. 93-02

Date of issue: 31 March, 1993

Publisher, Contact:
Hiroshi MATSUOKA
Planning Section, Administration Division
National Research Institute for Metals
2-3-12, Nakameguro, Meguroku, Tokyo 153, Japan
Phone+81-3-3719-2271 Fax+81-3-3792-3337

Printed by Tokyo Press Co., Ltd.

Basic Fatigue Properties of JIS Steels for Machine Structural Use

by

Satoshi NISHIJIMA

NRIM Special Report
(Technical Report)
No. 93-02

Contents